

UC Irvine

UC Irvine Previously Published Works

Title

Large-scale air mass characteristics observed over Western Pacific during summertime

Permalink

<https://escholarship.org/uc/item/6xq1j7xb>

Journal

Journal of Geophysical Research Atmospheres, 101(D1)

ISSN

0148-0227

Authors

Browell, EV
Fenn, MA
Butler, CF
[et al.](#)

Publication Date

1996

DOI

10.1029/95JD02200

Copyright Information

This work is made available under the terms of a Creative Commons Attribution License, available at <https://creativecommons.org/licenses/by/4.0/>

Peer reviewed

Large-scale air mass characteristics observed over Western Pacific during summertime

E. V. Browell,¹ M. A. Fenn,² C. F. Butler,² W. B. Grant,¹ J. T. Merrill,³
 R. E. Newell,⁴ J. D. Bradshaw,⁵ S. T. Sandholm,⁵ B. E. Anderson,¹ A. R. Bandy,⁶
 A. S. Bachmeier,² D. R. Blake,⁷ D. D. Davis,⁵ G. L. Gregory,¹ B. G. Heikes,³
 Y. Kondo,⁸ S. C. Liu,⁹ F. S. Rowland,⁷ G. W. Sachse,¹ H. B. Singh,¹⁰
 R. W. Talbot,¹¹ and D. C. Thornton⁶

Abstract. Remote and in situ measurements of gases and aerosols were made with airborne instrumentation to investigate the sources and sinks of tropospheric gases and aerosols over the western Pacific during the NASA Global Tropospheric Experiment (GTE)/Pacific Exploratory Mission-West A (PEM-West A) conducted in September-October 1991. This paper discusses the general characteristics of the air masses encountered during this experiment using an airborne lidar system for measurements of the large-scale variations in ozone (O₃) and aerosol distributions across the troposphere and airborne in situ instrumentation for comprehensive measurements of air mass composition. In low latitudes of the western Pacific the airflow was generally from the east, and under these conditions the air was observed to have low aerosol loading and low ozone levels throughout the troposphere. Ozone was found to be below 10 parts per billion volume (ppbv) near the surface to 40-50 ppbv in the middle to upper troposphere. In the middle and high latitudes the airflow was mostly westerly, and the background O₃ was generally less than 55 ppbv. On 60% of the PEM-West A flights, O₃ was observed to exceed these levels in regions that were determined to be associated with stratospheric intrusions. In convective outflows from typhoons, near-surface air with low ozone (<25 ppbv) was transported into the upper troposphere (>10 km). Several cases of continental plumes from Asia were observed over the Pacific during westerly flow conditions. These plumes were found in the lower troposphere with ozone levels in the 60-80 ppbv range and enhanced aerosol scattering. At low latitudes over the central Pacific the troposphere primarily contained air with background or low ozone levels; however, stratospherically influenced air with enhanced ozone (40-60 ppbv) was observed several times in the lower troposphere. The frequency of observation of the air masses and their average chemical composition are also discussed in this paper.

Introduction

The primary objectives of the NASA Global Tropospheric Experiment (GTE)/Pacific Exploratory Mission-West A (PEM-West A) field experiments were to investigate the atmospheric chemistry of ozone (O₃) and its precursors over the western Pacific, to examine the natural budgets of these species, and to assess the atmospheric impact of anthropogenic emissions [Davis *et al.*, this issue (a); Hoell *et al.*, this issue]. The first PEM-West mission focused on the late summer/early fall period (PEM-

West A) when the climatological flow in the lower troposphere of the western Pacific is expected to be predominantly from the east [Merrill *et al.*, 1985]. Under these flow conditions the air would have been over the remote Pacific for a long period of time. A second PEM-West mission was planned for the late winter to early spring period (PEM-West B) when a strong outflow from the Asian continent into the western Pacific is expected [Savoie and Prospero, 1989]. This is the season when the natural input of desert aerosols and the anthropogenic influence of Asia on the troposphere over the western Pacific is the largest. These two PEM-West missions represent the extreme conditions for determining the composition of the air and the tropospheric chemistry over the western Pacific.

The first instrumented aircraft study of the troposphere over the Pacific was Project GAMETAG (Global Atmospheric Measurements Experiment on Tropospheric Aerosol and Gases) conducted in August-September 1977 and April-May 1978 [Davis, 1980]. The GAMETAG program was designed to test models for short-lived photochemical species and provide survey data on a number of species over a latitude range from 70°N to 58°S. The latitudinal and vertical distribution of O₃ was studied, and anticorrelations were found between O₃ and water vapor (H₂O), suggesting a dynamical effect [Routhier and Davis, 1980]. These data were used in a modeling study which concluded that

¹Atmospheric Sciences Division, NASA Langley Research Center, Hampton, Virginia.

²Science Applications International Corporation, Hampton, Virginia.

³University of Rhode Island, Narragansett.

⁴Massachusetts Institute of Technology, Cambridge.

⁵Georgia Institute of Technology, Atlanta.

⁶Drexel University, Philadelphia, Pennsylvania.

⁷University of California, Irvine.

⁸Nagoya University, Toyokawa, Aichi, Japan.

⁹NOAA Aeronomy Laboratory, Boulder, Colorado.

¹⁰NASA Ames Research Center, Moffett Field, California.

¹¹University of New Hampshire, Durham.

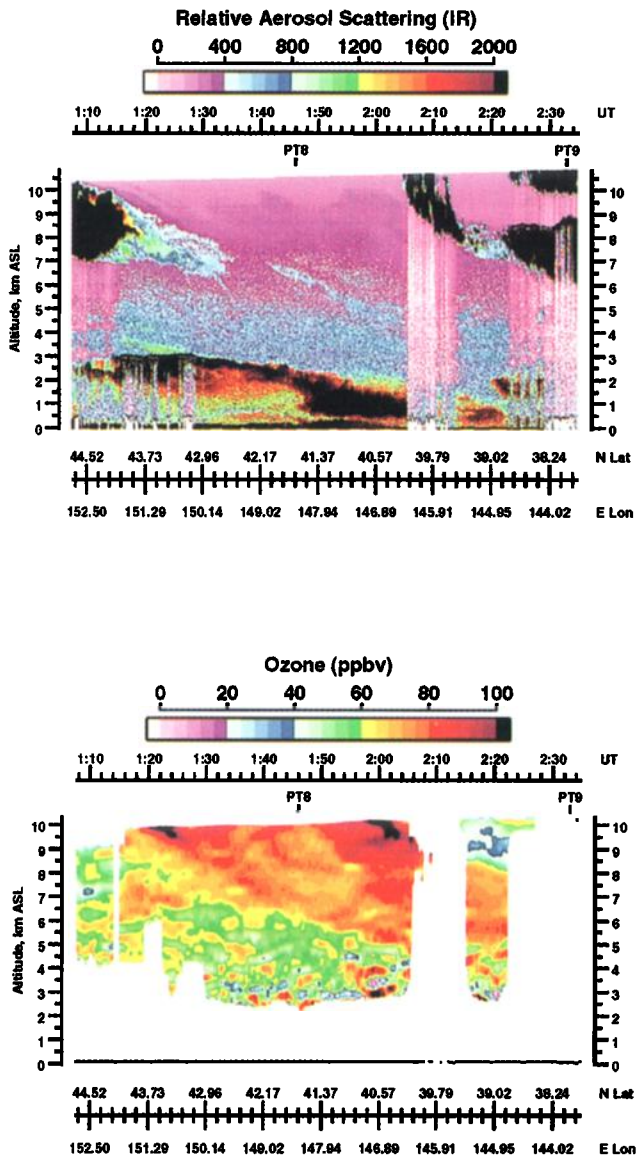
Anchorage to Yokota**PEM West-A Flight 5 18 Sep 91**

Plate 1. Aerosol (top) and O_3 (bottom) distributions obtained from nadir airborne DIAL measurements on September 18, 1991, over the western Pacific (east of Japan) on PEM-West A (PWA) survey flight from Anchorage, Alaska, to Yokota, Japan (PWA flight 5). The relative amount of atmospheric backscattering and O_3 mixing ratios in parts per billion by volume (ppbv) are defined by the color scales at the top of each display. Black represents values greater than the maximum level given on the color scale. Geometric altitudes are given in kilometers above sea level (ASL), and universal time (UT) is shown at the top of each display. Aircraft latitude and longitude information in degrees is given at the bottom of each display at each reference time.

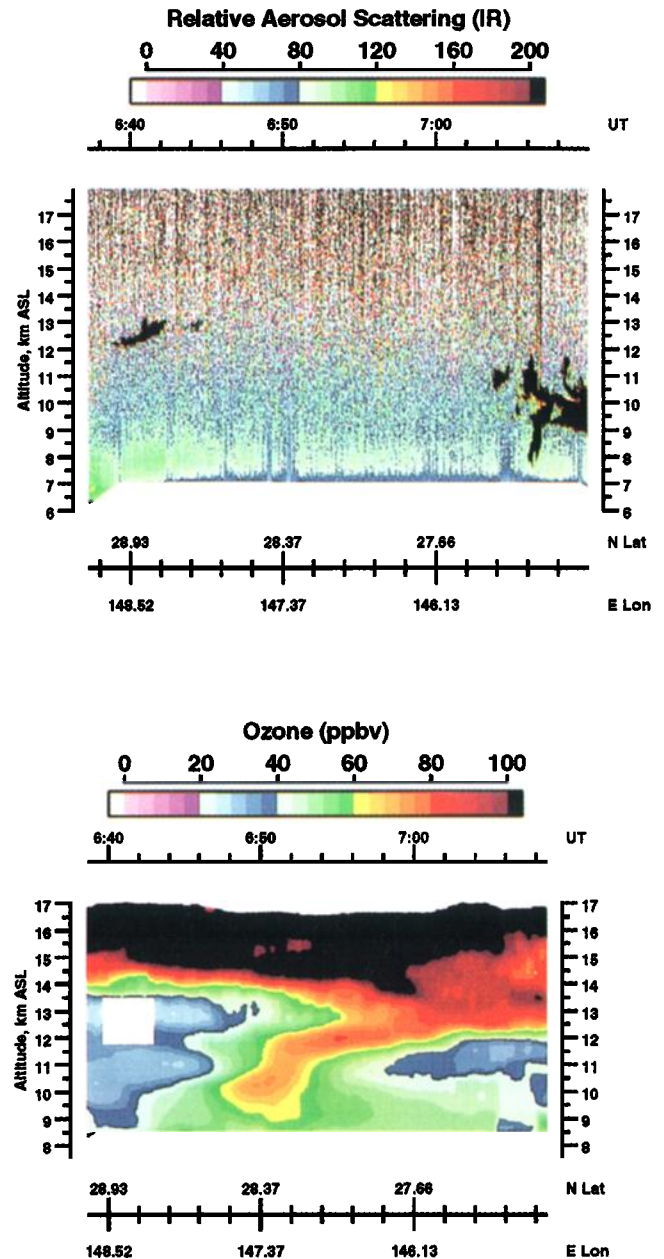
Marine-Wall**PEM West-A Flight 6 22 Sep 91**

Plate 2. Aerosol and O_3 distributions associated with a stratospheric intrusion observed in the upper troposphere southeast of Japan on September 22, 1991 (PWA flight 6).

Table 1. PEM-West A* Flight Information

Flight Number	1991	Mission	Latitude Range	Longitude Range
4	Sept. 16	survey (NASA Ames to Anchorage, Alaska)	37°N-61°N	154°W-122°W
5	Sept. 17	survey (Anchorage to Yokota, Japan)	35°N-61°N	140°E-150°E
6	Sept. 22	marine wall (southeast of Japan)	26°N-36°N	139°E-149°E
7	Sept. 24	continental wall (east of Japan)	35°N-42°N	139°E-149°E
8	Sept. 25-26	marine photochemistry (southeast of Japan)	27°N-36°N	139°E-147°E
9	Sept. 27	typhoon (south of Japan)	27°N-36°N	131°E-140°E
10	Oct. 1	survey (Yokota to Okinawa)	18°N-36°N	121°E-142°E
11	Oct. 2	survey (Okinawa to Hong Kong)	20°N-26°N	114°E-128°E
12	Oct. 4	continental outflow (east of Taiwan)	22°N-26°N	116°E-124°E
13	Oct. 6	Japanese flyby (south of Japan)	22°N-30°N	114°E-128°E
14	Oct. 8	survey (Hong Kong to Guam)	13°N-22°N	114°E-145°E
15	Oct. 10-11	ozone trough (southeast of Guam)	1°S-14°N	145°E-162°E
16	Oct. 13	high-pressure ridge (southwest of Guam)	4°N-14°N	125°E-145°E
17	Oct. 14-15	marine photochemistry (west of Guam)	13°N-16°N	138°E-145°E
18	Oct. 17-18	survey (Guam to Wake Island)	13°N-19°N	145°E-167°E
19	Oct. 18-19	survey (Wake Island to Hawaii)	15°N-21°N	167°E-158°W
20	Oct. 20	Mauna Loa flyby (Hawaii local)	18°N-21°N	158°W-154°W
21	Oct. 21-22	survey (Hawaii to Ames)	21°N-38°N	158°W-122°W

*Pacific Exploratory Mission-West A

O₃ in the equatorial Pacific was destroyed by a reaction between H₂O and O(¹D) and that odd nitrogen is deposited as nitric acid (HNO₃) and particulate nitrate (NO₃⁻) [Liu *et al.*, 1983]. One of the key findings from Project GAMETAG was the unusually large O₃ mixing ratios found in the troposphere between San Francisco and Hawaii, which led to further understanding of stratospheric injections of O₃ into the troposphere [Danielsen, 1980; Danielsen and Hipskind, 1980].

The NASA GTE/Chemical Instrumentation Test and Evaluation (CITE 2) aircraft mission was conducted in part over the northwestern Pacific in August 1986 [Hoell *et al.*, 1990]. The CITE 2 mission focused on intercomparison of techniques for measuring nitrogen dioxide (NO₂), nitric acid (HNO₃), and peroxyacetyl nitrate (PAN). In addition to establishing the measurement limitations of the various techniques, important new data were acquired on these and other species, including nitric oxide (NO), NO_y, O₃, carbon monoxide (CO), ethane (C₂H₆), and CFC-11 (CFCl₃) [Singh *et al.*, 1990] in clean air regions of the Pacific.

Measurements of the composition and chemistry in the lower troposphere over the Pacific were made as part of the NOAA Mauna Loa Observatory Photochemistry Experiment (MLOPEX) research program during May-June 1988. Downslope flow conditions at the Mauna Loa Observatory permit the sampling of air from the lower free troposphere, and measurements made during these periods have led to further the understanding of the distribution and photochemical interactions of reactive species in the remote marine troposphere [e.g., Ridley and Robinson, 1992].

The composition and chemistry of the marine boundary layer over the Pacific was studied as part of the Third Soviet-American Gas and Aerosol Experiment (SAGA 3) conducted in February-March 1990 over the western tropical Pacific aboard the former Soviet ship *Akademik Korolev* [Johnson *et al.*, 1993], and aerosols were studied off the coast of China on survey cruises from 1985 to 1987 by Zhou *et al.* [1992]. These ship measurements have provided extensive data sets on trace gases and aerosols in the marine boundary layer over the Pacific.

To study the budget of O₃ across the troposphere, we must be able to examine the sources and sinks of O₃ as they are related to

different air masses that are observed over the western Pacific. Contributions from stratosphere-troposphere exchange processes, natural photochemical processes, and anthropogenic photochemical processes must be examined across the entire troposphere to determine the large-scale magnitude of their impact on the tropospheric O₃ budget.

This paper reports the results of large-scale studies of the distribution of aerosols and O₃ over the western Pacific using primarily data from an airborne lidar system. These results, together with airborne in situ measurements of O₃ and aerosols [Gregory *et al.*, this issue], NO_x and NO_y [Smyth *et al.*, this issue], CO and methane (CH₄) [Gregory *et al.*, this issue], carbon dioxide (CO₂) [Anderson *et al.*, this issue], nitrous oxide (N₂O) [Collins *et al.*, this issue], sulfur dioxide (SO₂) and sulfate (SO₄) [Thornton *et al.*, this issue], PAN [Singh *et al.*, this issue], non-methane hydrocarbons (NMHC) [Blake *et al.*, this issue], hydrogen peroxide (H₂O₂) [Heikes *et al.*, this issue], and other species [Hoell *et al.*, this issue], and with the meteorological analyses of atmospheric transport [Bachmeier *et al.*, this issue; Merrill *et al.*, this issue; Newell *et al.*, this issue] provide insights into factors contributing to the summertime tropospheric distribution of O₃ and aerosols over the western Pacific.

Experimental Techniques

An airborne differential absorption lidar (DIAL) system was used to provide vertical profiles of O₃ and aerosols from near the surface to above the tropopause along the flight track of the NASA Ames Research Center (ARC) DC-8 aircraft. Simultaneous zenith and nadir lidar measurements of O₃ and aerosols were made from a range of about 750 m above and below the aircraft to above the tropopause in the zenith case and to about 300 m above the surface in the nadir case. The DIAL O₃ measurements were made using an on-line wavelength at 288.2 nm and the off-line wavelength at 299.5 nm, and the aerosol backscatter measurements were made at a laser wavelength of 1064 nm. An O₃ measurement accuracy of better than 10% or 2 ppbv (parts per billion by volume), whichever is larger, with a vertical resolution of 300 m in the nadir and 600 m

PEM-West (A) Mission Flight Tracks

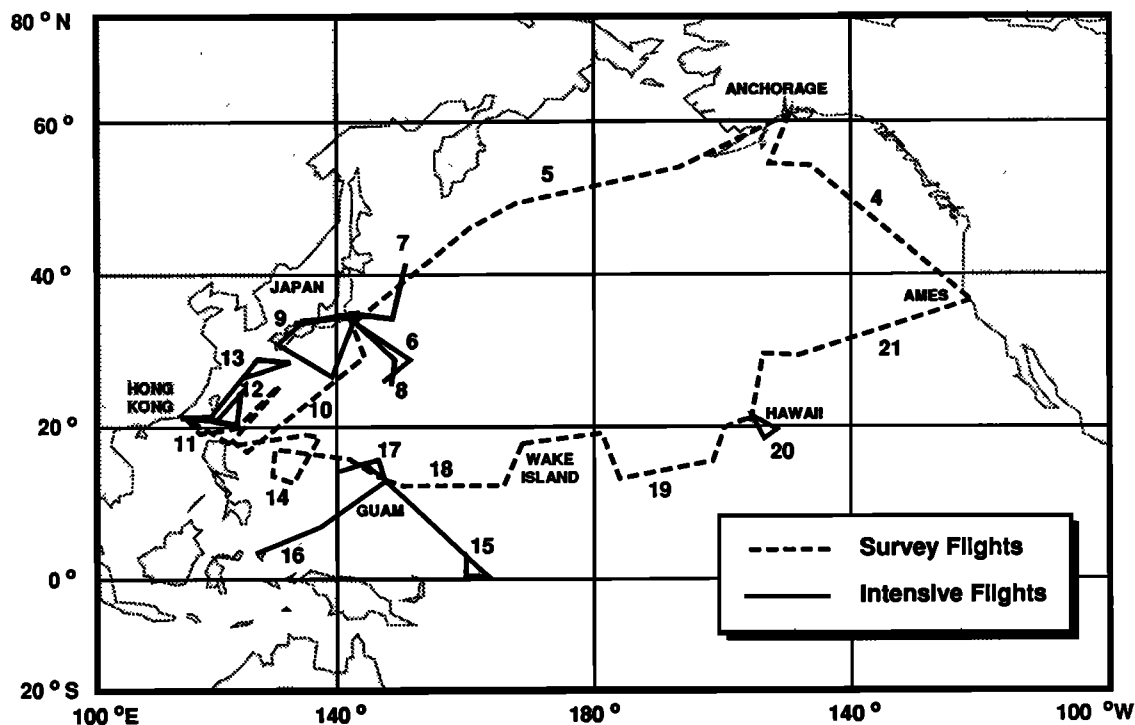


Figure 1. Map of PEM-West A (PWA) flight tracks with flight numbers shown.

in the zenith and a horizontal resolution in both cases of about 36 km (assuming a 3-min averaging time and an aircraft speed of 200 m/s) was obtained with a precision of better than 5% or 1 ppbv [Browell, 1983; Browell *et al.*, 1983, 1985a, b]. Comparisons between airborne DIAL and in situ O_3 measurements were made throughout PEM-West A to constantly verify that their agreement was consistent with the above stated limits. The aerosol backscatter measurements were derived from the range-corrected lidar signal at the 1064-nm laser wavelength, and the resolution of these measurements was defined by the vertical averaging interval of 60 m and the horizontal averaging interval of 1.75 s or about 350 m. The accuracy and precision of the aerosol measurements were better than 1%. Detailed characteristics of the current airborne DIAL system and the O_3 DIAL technique are given by Browell [1989].

In addition to the airborne DIAL system the DC-8 had instrumentation for in situ measurements of O_3 , aerosol size distribution, aerosol number density, NO_x , NO_y , CO, CH_4 , N_2O , SO_2 , SO_4 , HNO_3 , PAN, NMHCs, CFCs, H_2O_2 , 7Be , other trace species, and meteorological parameters such as temperature, dew point, and winds. A general description of these systems and their measurements is given by Hoell *et al.* [this issue], and more details are provided in companion papers in this issue.

Data Results and Discussion

Eighteen missions were conducted as part of the PEM-West A field experiment between September 16 and October 21, 1991. A list of the PEM-West A missions, the mission objectives, and the latitude and longitude ranges of the missions are given in Table 1, and the flight tracks for these missions are shown in Figure 1. During this field experiment, eight flights were survey missions

between NASA ARC, Anchorage, Alaska, Yokota, Japan, Okinawa, Hong Kong, Guam, Wake Island, Hawaii, and NASA ARC; and ten flights were "local" missions for intensive measurements over the Pacific from the bases in Japan, Hong Kong, Guam, and Hawaii.

Ozone and aerosol distributions were measured remotely with the DIAL system on all flights during PEM-West A. These measurements provided nearly complete altitude coverage of O_3 and aerosol distributions from near the surface to the tropopause region along the aircraft flight track.

The air masses observed during PEM-West A were broadly divided into six main categories: background air in the free troposphere, near-surface (mixed layer) air, stratospherically influenced air, convective outflows, plumes, and clean Pacific air. Examples are presented below for the O_3 and aerosol distributions that were observed during PEM-West A (PWA). Characteristics are discussed for the different types of air masses, and an analysis is given of the extent to which the air masses were observed in various regions of the Pacific in different altitude ranges. The average O_3 profile and chemical composition of major air mass types are also presented.

Ozone Enhancement from Stratospheric Intrusions and Continental Outflow

The survey flight from Anchorage, Alaska, to Yokota, Japan, on September 18, 1991 (PWA flight 5), revealed the presence of extensive stratospheric intrusions that extended down into the lower troposphere (<5 km) at midlatitudes over the western Pacific. Plate 1 shows the aerosol and O_3 distribution observed east of Japan on that flight. An air mass with relatively low aerosol scattering (<200) and high O_3 mixing ratios (>60 ppbv)

can be seen in the center of Plate 1. This air mass is bounded by air with enhanced aerosol scattering (>400) that sometimes exceeds the scattering in the clean regions by an order of magnitude (>2000) and is optically thick in some locations (note attenuation of lidar signals in those regions). There are also enhanced O_3 levels (>50 ppbv) in association with the enhanced aerosol regions below ~ 6 km. The upper level (>6 km) aerosol layers are clouds, and they are associated with intermediate levels of O_3 (30–50 ppbv).

The in situ measurements on the DC-8 indicated that we were flying in the lower stratosphere at 11 km along this flight track. The highest values of O_3 (262 ppbv) were obtained at 0111 UT, and at that time the dew point (DPT) was -66°C ; CO was 52 ppbv; CH_4 was 1670 ppbv; N_2O was 300 ppbv; SO_2 was 226 pptv (parts per trillion by volume); SO_4 was 208 pptv; NO was 30 pptv; NO_y was 593 pptv; ^7Be was 2653 fCi/m 3 ; and PAN was 116 pptv at 0108 UT. The levels of SO_2 and SO_4 were elevated due to the injection of gases and aerosols into the lower stratosphere from the Mount Pinatubo eruption that occurred in the Philippines in June 1991. The zenith DIAL measurements showed that O_3 continued to increase above the aircraft, further confirming that we were in the lower stratosphere. The air mass below us with the elevated O_3 and the relatively low aerosol scattering (compared to the tropospheric aerosol loading) appeared to be an extension of the air mass we were flying in at 11 km. A cross section of potential vorticity (PV) derived from the European Center for Medium-Range Weather Forecasting (ECMWF) meteorological analysis for a portion of our flight track and within 2 hours of our time is shown in Figure 2. The PV analysis confirmed the intrusion of air with enhanced PV levels ($>4 \times 10^{-7} \text{ deg m}^2 (\text{kg s})^{-1}$) extending down to ~ 3 km near

40°N and the sampling of the aircraft in the lower stratosphere at ~ 250 hPa (PV ~ 20). The vertical and horizontal extent of the intrusion was clearly evident in the airborne DIAL data south of 50°N , and there was good correlation between the O_3 enhanced regions and the PV analysis. Large-scale stratospheric intrusions have been observed previously with an airborne lidar at midlatitudes in the spring [Browell et al., 1987] and at high latitudes in the summer [Browell et al., 1992, 1994]; however, this was the first observation of this large-scale transport process at midlatitudes in the summer.

An air mass backtrajectory was calculated to determine the origin of the air mass with enhanced aerosols and enhanced O_3 below ~ 6 km. The wind analysis along the flight track on September 18, 1991, indicated that the air mass with enhanced aerosols below ~ 6 km (Plate 1) was coming off the Asian continent, and the enhanced O_3 was thought to be due to photochemical O_3 production from precursor gases released over Asia. Air mass backtrajectories were computed for four altitudes (1.5, 4, 10, and 14 km) where different air mass characteristics were observed at 0150 UT on flight 5 (Figure 3). The air in the lowest layer, which has the most aerosols, came south from western Russia before turning southeast over China and Japan. The 4-km layer came east from the middle of Russia, and the higher layers came directly east over the Asian continent. These results confirm that the air with enhanced aerosols and O_3 had a continental source.

A second example of a stratospheric intrusion observed during PEM-West A southeast of Japan is shown in Plate 2. In this case, the intrusion was observed to extend down from a tropopause height of about 14.5 km on the northern side of the intrusion (left side of plate) to below 9 km in the upper troposphere. The intru-

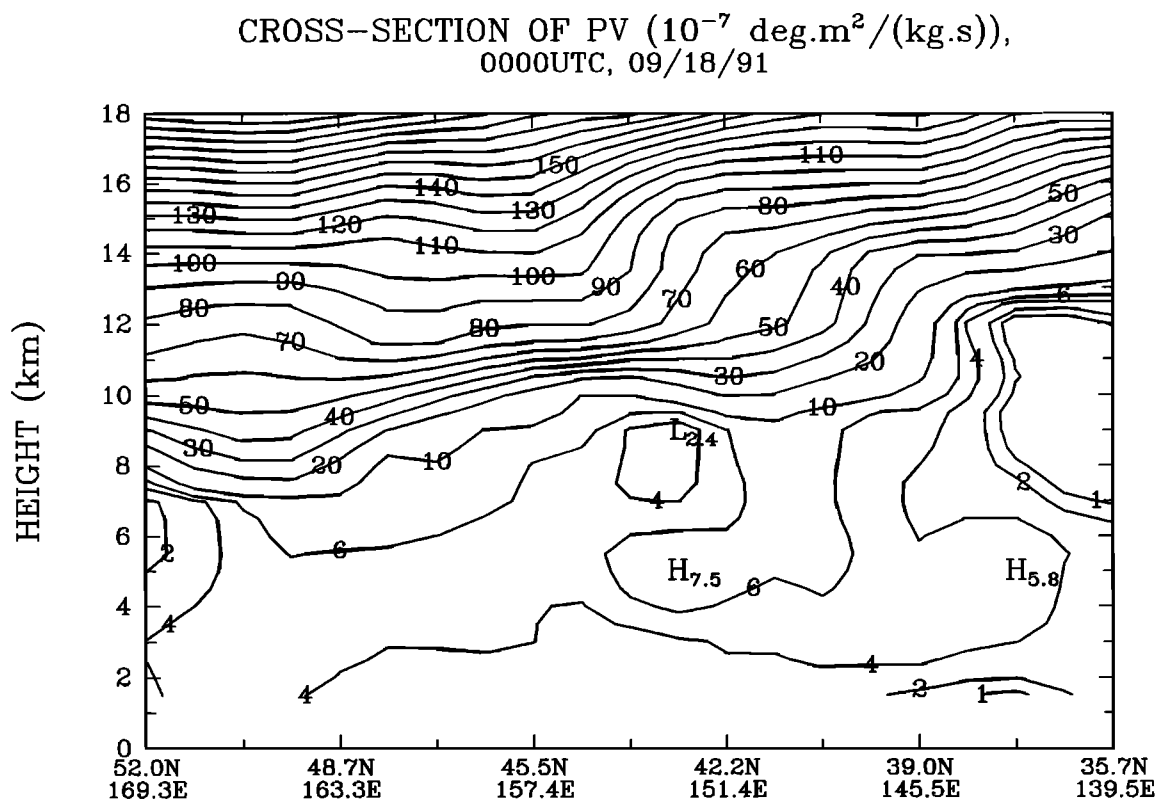


Figure 2. Cross section of potential vorticity ($10^7 \text{ deg m}^2 (\text{kg t})^{-1}$) at 0000 UT on September 18, 1991, along portion of flight track of DC-8 on PWA flight 5.

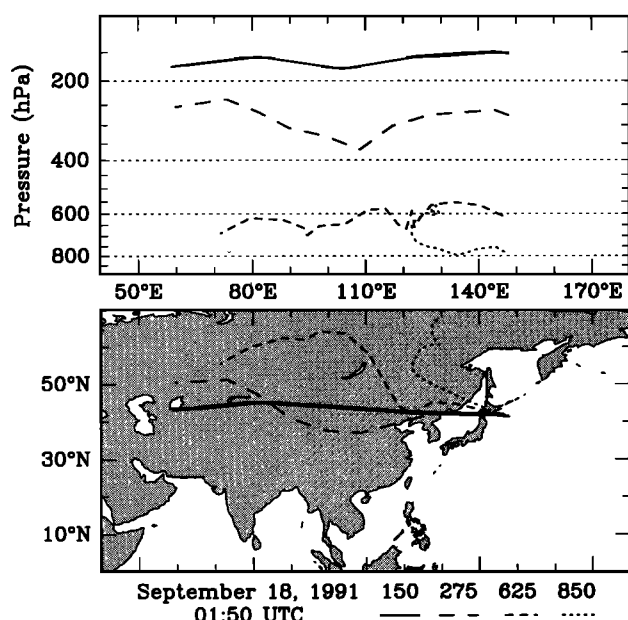


Figure 3. Isentropic backtrajectory analysis starting from 41°N/148°E at 0150 UT on September 18, 1991 (PWA flight 5), at 150 hPa (~14 km) (solid line), 275 hPa (~10 km) (long-dashed line), 625 hPa (~4 km) (medium-dashed line), and 850 hPa (~1.5 km) (short-dashed line). Pressure levels (top) and geographic locations (bottom) of the various air parcels are shown for a total of 10 days in the backtrajectory.

sion also has relatively low aerosol loading in the region of the enhanced O_3 . Unlike the large intrusion (>800 km in horizontal extent) shown in Plate 1, the intrusion shown in Plate 2 was not resolved in the ECMWF PV analysis due to its limited size (<150 km in horizontal extent). The aerosol distribution also shows the presence of thin cirrus clouds on either side of the intrusion. The air in the vicinity of the cirrus has low O_3 (typically <40 ppbv) associated with it. Since the moisture to form the cirrus clouds is being pumped into the upper troposphere from near the ocean surface by deep convection associated with typhoons [Newell *et al.*, this issue], the lower levels of O_3 that are near the surface are also transported into this region. This topic will be discussed in more depth in a section below.

A continental outflow from Asia was investigated east of Japan on September 24, 1991 (PWA flight 7). Plate 3 shows the aerosol and O_3 distributions observed over the western Pacific on that mission. Significant amounts of aerosols were observed in the outflow region below 8 km (see left side of Plate 3). Except for the near-surface air (<2 km) the O_3 generally exceeded ~50 ppbv in the enhanced aerosol air masses, and in some areas, O_3 exceeded 70 ppbv. There was large variability in the aerosol scattering and O_3 levels near the surface with values ranging from 30 to 75 ppbv. In regions above 6 km the amount of aerosol scattering was reduced from the aerosol loading in the lower troposphere; however, the O_3 levels were as high or higher than in the aerosol-enhanced layers. The zenith measurements are shown with a more sensitive aerosol-scattering scale, and while the level of aerosol scattering is reduced, there are some aerosols clearly present below 11 km where O_3 exceeds 100 ppbv in some regions. The enhanced O_3 with low aerosol loading above ~12 km is associated with stratospheric air. The tropopause (as indicated by the O_3 =100 ppbv level) decreases in altitude from

15.5 km at ~35°N to 12 km at ~42°N with enhanced O_3 below the tropopause indicating a broad transition region of mixing between the stratosphere and the troposphere. Evidence of cirrus clouds with lower O_3 (<40 ppbv) can also be seen between 9.5 and 12.5 km. A backtrajectory analysis is presented in Figure 4 for selected altitudes at 0450 UT in this flight. This analysis clearly shows that the flow was from the west at all altitudes bringing gases and aerosols over the Pacific from China and Japan.

The aerosol and O_3 distributions shown in Plate 4 were obtained on October 6, 1991, near Taiwan. The aerosol distribution below 6 km indicated that some portion of the air resulted from a continental outflow; however, the O_3 distribution only showed enhanced O_3 associated with the heavier aerosol loading region below about 3.5 km. Low O_3 (<20 ppbv) was observed in part of the light aerosol scattering region from the 3.5- to the 5.5-km region, and above ~5.5 km to the tropopause at ~16.5 km the O_3 ranged from 40 to >100 ppbv in what appeared to be relatively clean air (low aerosol loading). The backtrajectory analysis done for this case (Figure 5) showed that the low-altitude air (~3 km) traveled over portions of the ocean and land areas before arriving at our measurement location. The low O_3 component of the air resulted from the marine portion of the trajectory, and the enhanced aerosols and O_3 came from inputs from either Taiwan and/or from the coast of China. The clean air with elevated O_3 came from over China with the air at ~6 km descending from ~9 km during the trajectory. While the low aerosol loading and enhanced O_3 levels of these air masses are consistent with the characteristics of stratospheric intrusions discussed above, the PV analysis did not show evidence for a stratospheric intrusion that would explain the magnitude of the O_3 enhancement that was observed. Clouds associated with deep convection (>12 km) over China were observed from the aircraft during this flight, and in situ measurements of air mass composition at ~9 km confirmed that the air was not of stratospheric origin. Large aerosols can be washed out of the air during the deep convective events [Gatz, 1977], while insoluble gases will pass into the outflow region in the middle to upper troposphere to photochemically produce O_3 if the precursor gases are present [Pickering *et al.*, 1989, 1991].

This discussion has presented examples of the major processes that were observed to increase O_3 in the troposphere over the western Pacific during PEM-West A. These processes include stratospheric intrusions which mix elevated concentrations of O_3 with the background tropospheric air to produce what we call stratospherically influenced air, and continental outflows which can increase O_3 if the precursor gases are present in the air that is directly advected over the Pacific in aerosol-laden plumes or in outflows from convection over the continent.

Low Ozone Air and Convective Transport over Pacific

The first observation of an extensive region of air containing low O_3 (<30 ppbv) was on October 1, 1991, on a survey flight that was originally planned to go from Yokota, Japan, to Hong Kong, but because of a problem with the weather radar on the DC-8 and the presence of Typhoon Nat over the South China Sea was diverted to Okinawa. Plate 5 presents the aerosol and O_3 distributions observed east of the northern tip of the Philippines on this flight. Except for the aerosols contained predominantly in the marine boundary layer below ~1.5 km and some cloud activity seen on the right of the cross section, the atmosphere was clean of aerosols below ~11.5 km. The region of low O_3 (<30 ppbv) extended from the marine boundary layer to just

Continental Wall

PEM West-A

Flight 7

24 Sep 91

Aerosol Data

Ozone Data

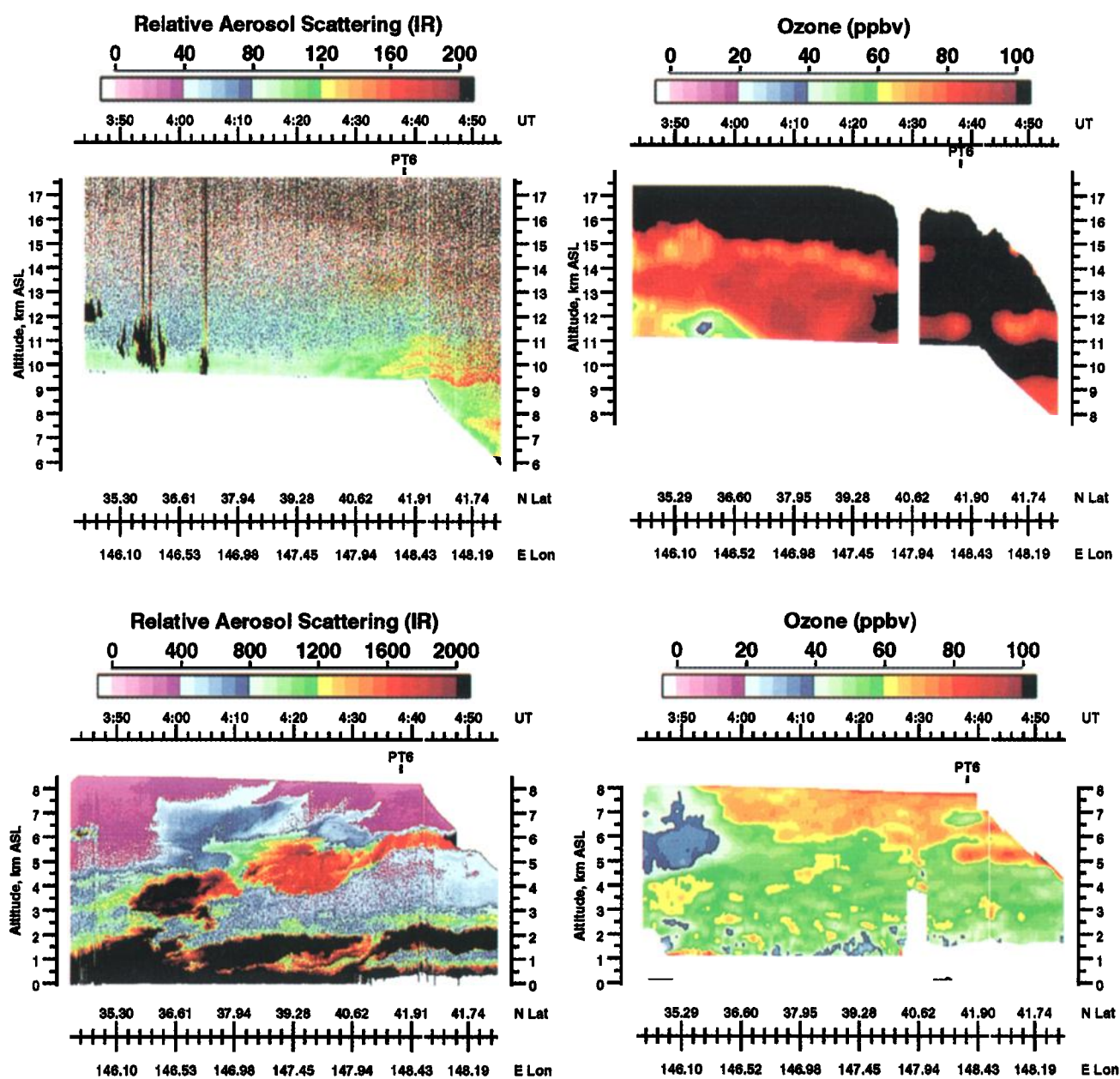


Plate 3. Aerosol (left side) and O₃ (right side) distributions in the continental outflow observed east of Japan on September 24, 1991 (PWA flight 7).

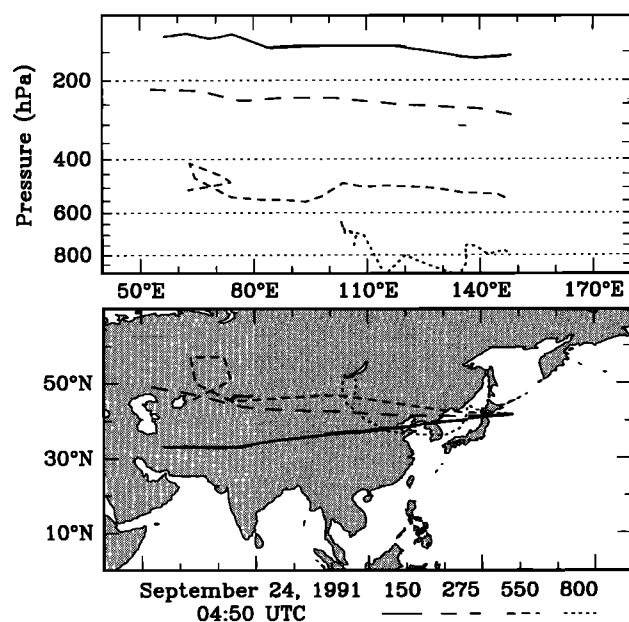


Figure 4. Backtrajectory analysis for 10 days starting from 41.7°N/148°E at 0450 UT on September 24, 1991 (PWA flight 7), at 150 hPa (~14 km) (solid line), 275 hPa (~10 km) (long-dashed line), 550 hPa (~5 km) (medium-dashed line), and 800 hPa (~2 km) (short-dashed line).

below the tropopause at ~16 km. There were also regions where O_3 was less than 20 ppbv over most of the depth of the troposphere. An extensive region of cirrus with a depth of ~4 km was observed just below the tropopause, and the O_3 associated with it was typical of the O_3 values near the surface. Figure 6 shows the backtrajectories for three representative altitudes in Plate 5. While the trajectories at the different altitudes are from different directions due to the variations in wind patterns with altitude around Typhoon Nat, they have the common characteristic of spending the last 10 days over the water at low latitudes. While the 800 and 475 hPa air parcels were probably in the inflow region of the typhoon, the 200-hPa level was in the outflow region of the typhoon as indicated by the presence of extensive cirrus clouds in the upper troposphere. For more discussion of typhoon dynamics and its implications for atmospheric chemistry, see Newell *et al.* [this issue].

On the flight southeast of Guam into the "ozone trough" on October 11, 1991 (PWA flight 15), the lowest O_3 levels were observed. The nadir and zenith O_3 distributions obtained near the equator are shown in Plate 6. In this case, O_3 was less than 10 ppbv below 3 km, less than 25 ppbv up to 13 km, and less than 35 ppbv up to 15 km. A region of even lower O_3 was observed between 6° and 10°N where O_3 was less than 15 ppbv from near the surface to above 11 km. The backtrajectory analysis for representative altitudes at 0240 UT is shown in Figure 7. At all altitudes the flow was from the east, and the air parcels had been over the Pacific for at least 10 days. Photochemical destruction of O_3 over the tropical Pacific due to hydroxyl (OH) chemistry is thought to be the cause of these very low O_3 levels [see Davis *et al.*, this issue (b)].

Tropospheric Occurrence of Different Air Masses

To assess the relative impact of various air mass types on determining the composition of the troposphere over the Pacific,

the nadir and zenith DIAL O_3 and aerosol data were used to categorize the air mass types observed on all flights during PEM-West A. Prior to establishing the criteria for the different air mass types, a reference or background O_3 profile had to be defined. The reference O_3 profile shown in Figure 8 is an approximation to the average of a series of O_3 profiles that were selected to be representative of air that was reasonably unaffected by recent sources/sinks of O_3 and aerosols. While the reference O_3 profile may be close to the average western Pacific midlatitude background O_3 profile, it is really only a model for use as a discriminator in this analysis. A better estimate of the average background O_3 profile will come from the air mass analysis to be discussed below.

Nine air mass types were identified during this field experiment, and they were categorized using the following criteria in each altitude range: (1) background or reference air (BKG/REF) in the free troposphere, O_3 within 80-120% of reference O_3 profile and low aerosol scattering (within factor of 2 of estimated scattering from aerosol-free region at same altitude); (2) near-surface air (NS), enhanced aerosol scattering (more than factor of 2 of estimated scattering from nearby aerosol-free region) below about 2 km and O_3 less than 120% of reference O_3 profile; (3) plumes with low O_3 in the free troposphere (LPLU), enhanced aerosol scattering and O_3 less than 80% of reference O_3 profile; (4) plumes with background O_3 in the free troposphere (BPLU): enhanced aerosol scattering and O_3 within 80-120% of reference O_3 profile; (5) plumes with high O_3 in the free troposphere (HPLU), enhanced aerosol scattering and O_3 greater than 120% of reference O_3 profile; (6) clean Pacific air (CP), O_3 less than 80% of reference O_3 profile and low aerosol scattering; (7) stratospherically influenced air (SINF), O_3 more than 120% of reference O_3 profile and aerosol scattering comparable to levels above the tropopause; (8) convective outflows from convection over the ocean (CO), O_3 less than 80% of reference O_3 profile

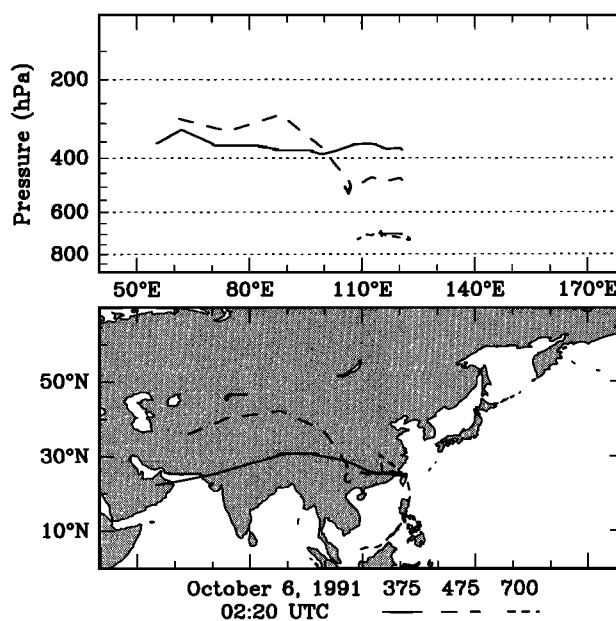


Figure 5. Backtrajectory analysis for 10 days starting from 24.5°N/121°E at 0220 UT on October 6, 1991 (PWA flight 13), at 375 hPa (~8 km) (solid line), 475 hPa (~6 km) (long-dashed line), and 700 hPa (~3 km) (medium-dashed line).

Japanese Flyby

PEM West-A

Flight 13

6 Oct 91

Aerosol Data

Ozone Data

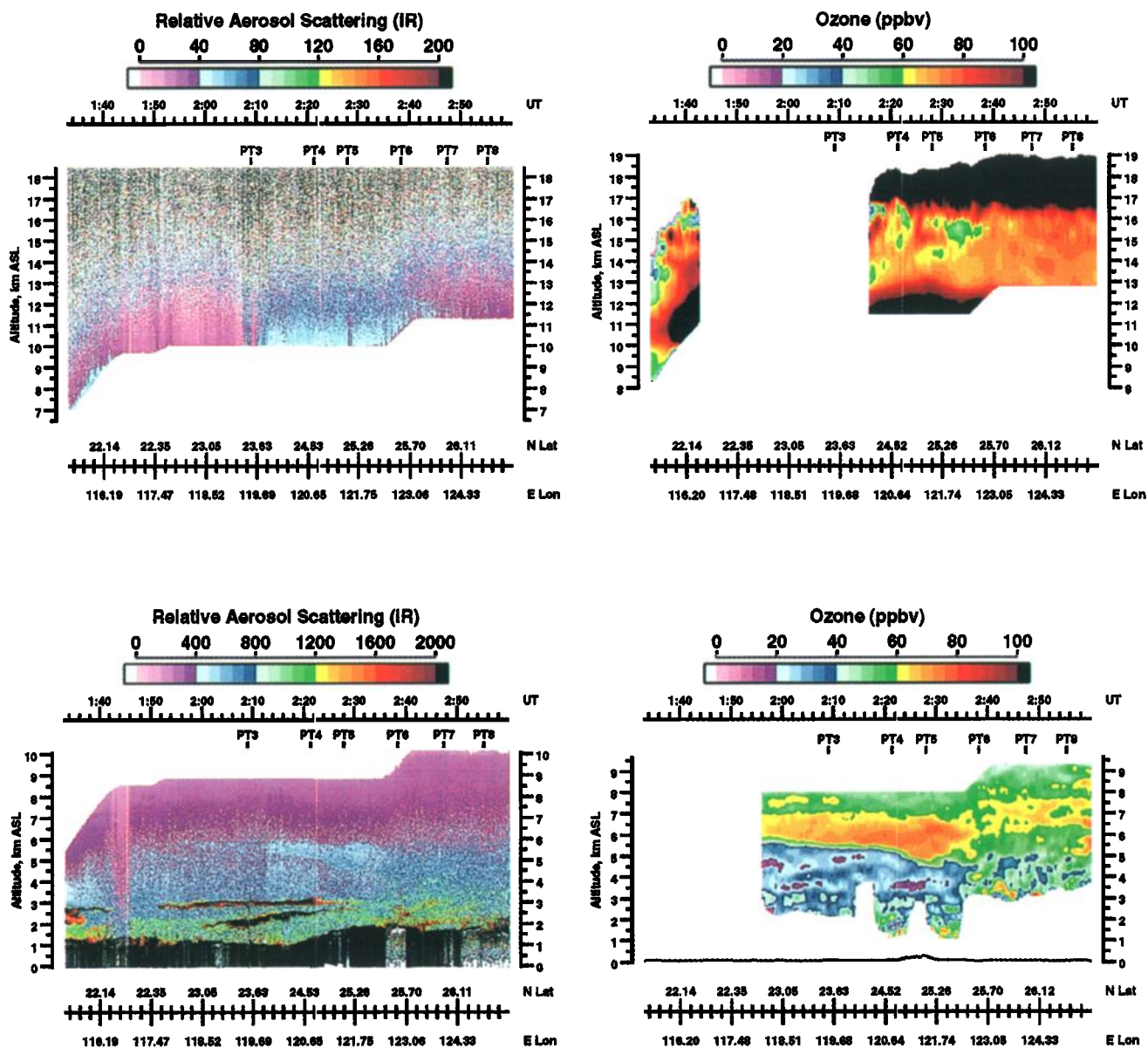


Plate 4. Aerosol and O₃ distributions associated with convective outflow from the continent observed near Taiwan on October 6, 1991 (PWA flight 13).

Yokota to Okinawa

PEM West-A

Flight 10

1 Oct 91

Aerosol Data

Ozone Data

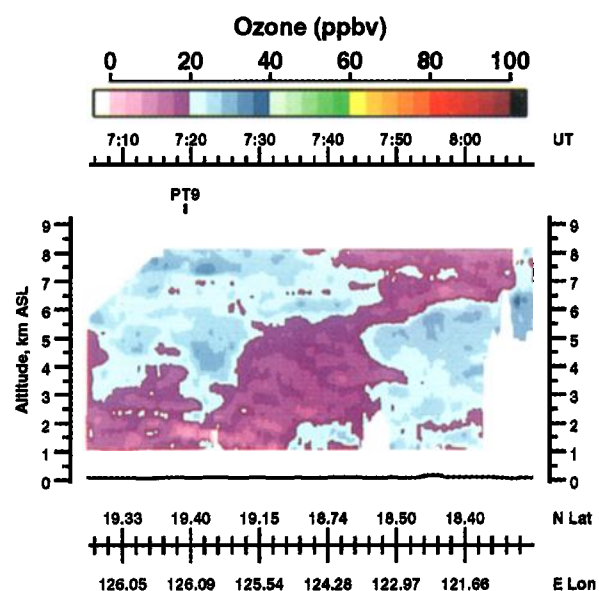
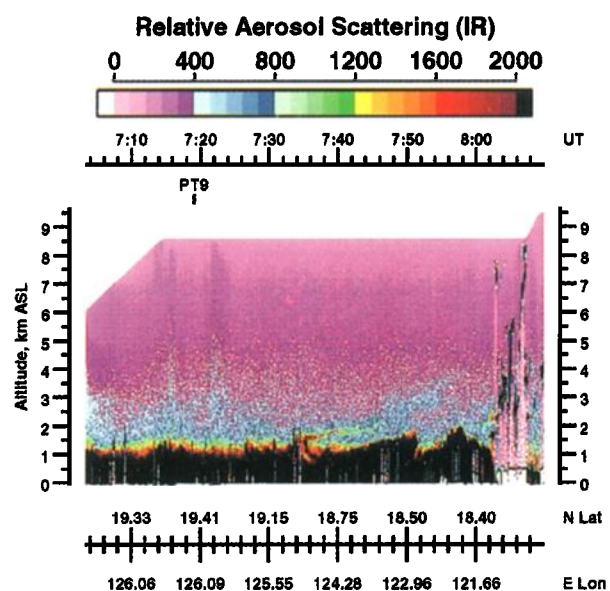
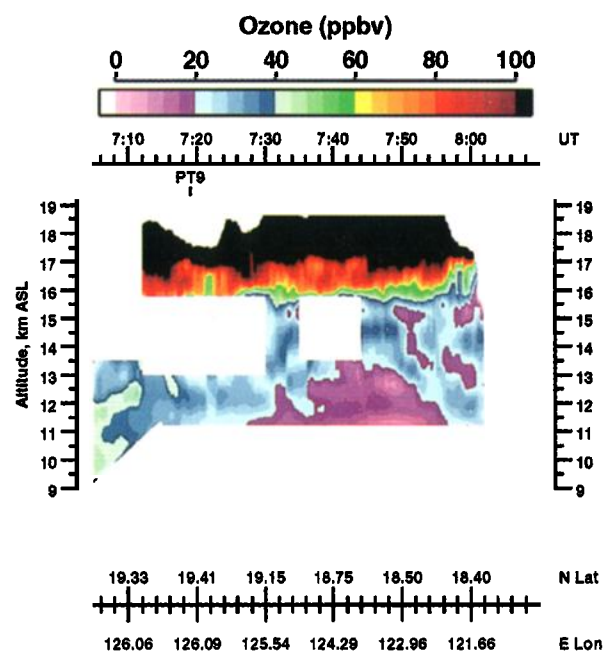
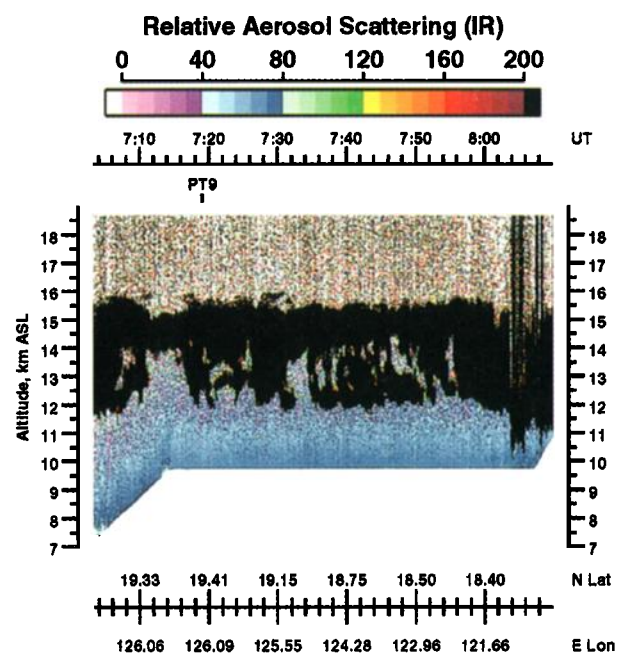


Plate 5. Aerosol and O₃ distributions associated with clean Pacific air and convective outflow observed near Taiwan on October 1, 1991 (PWA flight 10).

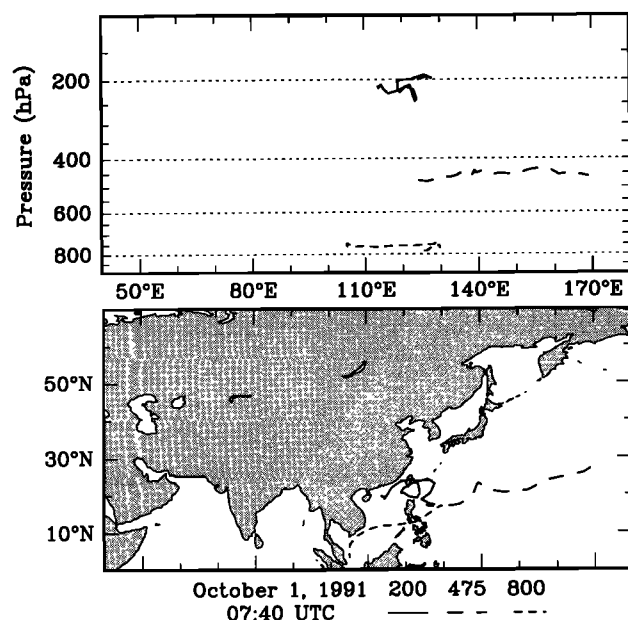


Figure 6. Backtrajectory analysis for 10 days starting from 19°N/124°E at 0740 UT on October 1, 1991 (PWA flight 10), at 200 hPa (~12 km) (solid line), 475 hPa (~6 km) (long-dashed line), and 800 hPa (~2 km) (medium-dashed line).

and in vicinity of cirrus clouds; (9) convective outflows from convection over the continent (CO-C), O_3 more than 120% of reference O_3 profile, low aerosol scattering, and no evidence of stratospheric intrusions in PV analysis.

The results of the air mass analysis are presented in Plate 7. At high latitudes (40°–60°N) over the Pacific the average tropopause was at an altitude of ~8 km (>70% of SINF were above this altitude). This is also confirmed by the average O_3 profile for the SINF for this region (Figure 9) where the average O_3 at 8 km exceeded 80 ppbv. A significant percentage of the troposphere above 6 km ($\geq 20\%$) consisted of SINF and the balance of the troposphere was mainly composed of plumes with enhanced O_3 from continental outflows. The average O_3 profile for these plumes was 17–20 ppbv (~45%) greater than the reference O_3 profile (Figure 9). Less than 25% of the troposphere consisted of plumes with background O_3 levels. In this latitude range the main flow was from the Asian continent over the Pacific throughout the troposphere.

At midlatitudes (20°–40°N) over the western Pacific the average tropopause was at ~16 km, and the background air was the predominant air mass type throughout the free troposphere, representing about 40% of the troposphere from 3 to 16 km. This provides confirmation that the O_3 reference profile used in the air mass classifications does represent the average air mass type in this region. In addition, the average O_3 profile for this air mass type was very close to the reference O_3 profile chosen for the air mass discrimination (Figure 10). The SINF and convective outflows (marine) also contributed greatly to the composition in the upper troposphere. In the midtroposphere, many different air mass types were observed, and in the lower troposphere, plumes from continental outflows and convective outflows from the continent were the dominant air masses. Figure 10 shows the average O_3 profiles for these air masses in the midlatitude region. The high O_3 plumes had up to 100% higher O_3 than that found in

the background air, and in the upper troposphere the O_3 in the SINF was ~40% higher than the background average. The O_3 levels in the convective outflows (marine) were comparable to O_3 levels 5 to 10 km lower in the troposphere.

The results for the western Pacific low-latitude region show that the tropopause was typically above 16 km and that outflows from convection over the ocean were present a large percentage of the time in the upper troposphere. The low O_3 associated with the clean Pacific air and convective outflows dominated the air masses in the southwestern Pacific. Figure 11 shows the average O_3 profiles for these two dominant air mass types. The O_3 in the clean Pacific air near the surface was less than 9 ppbv, which is more than 50% lower than the O_3 reference profile, and in the middle to upper troposphere, the low O_3 air in outflows was typically ≤ 33 ppbv, which is about 50% lower than the reference profile. Only a low percentage of plume cases were observed in this region, and they were mostly below 5 km. Background air mass conditions were found in a low percentage of observations (5–15%) across the troposphere.

In the central Pacific at low latitudes the tropopause was typically between 15 and 16 km, and background air was the main air mass type observed in the middle to upper troposphere. In spite of the high percentage of observations of background air in this region, the average O_3 profile was strongly influenced by the convective outflow (marine) air below the tropopause (Figure 12), and in the lower troposphere the average O_3 profile was a combination of clean Pacific, background, and SINF air mass types. Clean Pacific air was found on average of about 50% of the time below 9 km, and the amount of background air decreased with decreasing altitude in this region. The average O_3 profile for the clean Pacific air in the central Pacific was within 20% (~4 ppbv) of the same air mass in the western Pacific (Figure 11). A few plumes were observed below 4 km with enhanced O_3 in them. These plumes were advected into this region from biomass burning that was occurring on Borneo. The observation of SINF

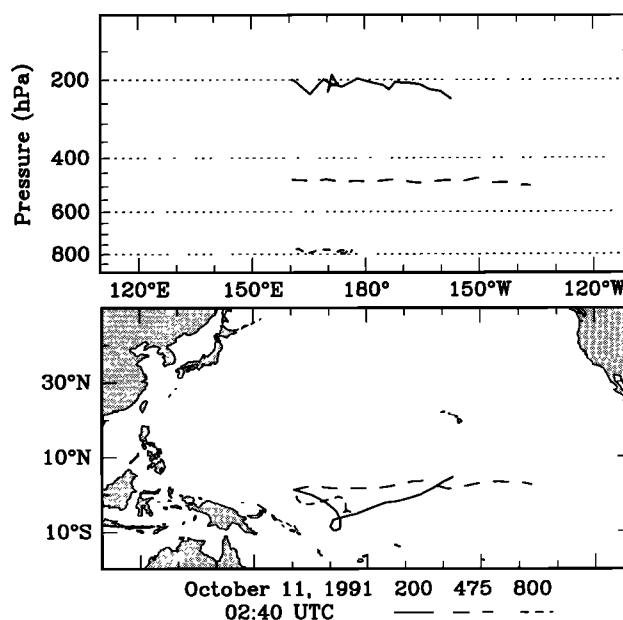


Figure 7. Backtrajectory analysis for 10 days starting from 1.3°N/161°E at 0240 UT on October 11, 1991 (PWA flight 15), at 200 hPa (~12 km) (solid line), 475 hPa (~6 km) (long-dashed line), and 800 hPa (~2 km) (medium-dashed line).

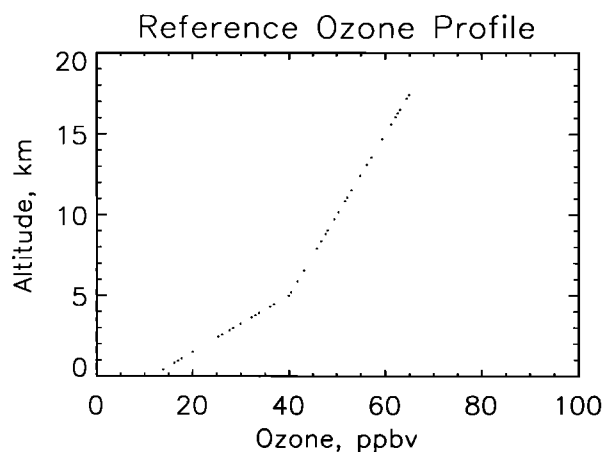


Figure 8. Reference O_3 profile used in air mass characterization analysis.

in the lower troposphere came as a surprise. This air was transported from stratospheric intrusions at midlatitudes over the western Pacific to the low latitudes of the central Pacific by advection and descent around the climatological high-pressure system typically situated in the southwestern Pacific [Bachmeier *et al.*, this issue]. This is the reason why no SINF was observed in the upper troposphere in this region. The O_3 increased by as much as 110% in the lower troposphere due to the transported air from the stratosphere compared to the background O_3 levels.

Tables 2-4 present summaries of the regional and altitude dependence of several major air mass types observed during PEM-West A. The distribution of SINF is shown in Table 2. The latitude dependence of the tropopause levels and the frequency of occurrence of enhanced O_3 due to stratospheric intrusions are clearly seen in this table. A significant tropospheric extent of SINF at midlatitudes over the Pacific was observed with generally increasing frequency with altitude and covering an average of more than 39% of the troposphere above 9 km. The amount of SINF in the upper troposphere (>6 km) at high latitudes and in the lower troposphere (<5 km) at low latitudes over the central Pacific is given in this table. Table 3 gives the total percentage of the troposphere that contains all plume types. The amount of plumes below 8 km increased with increasing latitude over the western Pacific. This was predominantly the result of the advection of boundary layer continental air over the Pacific as a result of the climatological high-pressure system that is present in the southwestern Pacific during the summer. Some plumes in the lower troposphere were also observed in the central Pacific as a result of long-range transport in the 2- to 4-km range over thousands of kilometers into the central Pacific. The low O_3 air, as represented by the clean Pacific air and convective outflow (marine) air (Table 4), consisted of 55-95% of the entire troposphere from 2-15 km at low latitudes in the western Pacific to 35-66% in the same altitude range in the central Pacific. At midlatitudes the extent of low O_3 air was reduced to 18-38% in the 4- to 14-km range, and there was negligible evidence of low O_3 air in the high-latitude region.

The average percentage of the troposphere that contains the different air mass types in the different locations is given in Table 5. In the low latitudes of the western Pacific the low- O_3 air (clean Pacific and convective outflow marine air) represented 68% of the troposphere, while the background conditions (free troposphere and near-surface air) was 14%. In the central Pacific

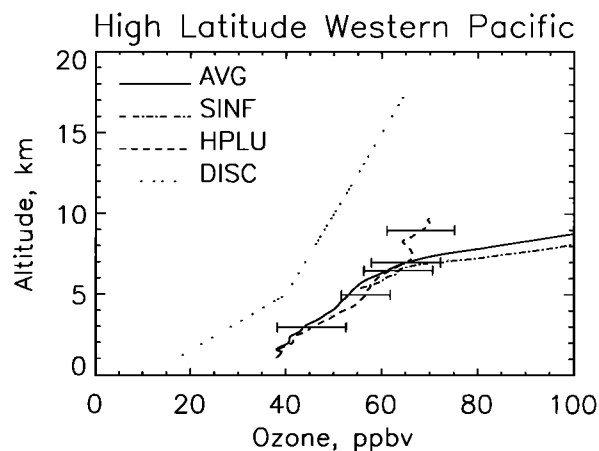


Figure 9. Average O_3 profile for Pacific high latitude (40° - 60° N/ 150° E- 160° W) region (solid line), and average O_3 profiles for stratospherically influenced air (large-short-dashed line) and plumes with enhanced O_3 (long-dashed line) shown relative to the reference O_3 profile, or discriminator (short-dashed line). Horizontal bars represent the standard deviation of the measurements for each air mass type.

the low- O_3 air was 37% of the troposphere and the background was 46%. At midlatitudes the enhanced- O_3 air (enhanced- O_3 plumes and SINF) and the background air were both 36% of the troposphere. At high latitudes the enhanced- O_3 air comprised most of the troposphere with 64% in plumes and 27% in SINF.

Contribution of Different Air Masses to Ozone Budget

The fractional contribution of the different air mass types to the O_3 budget in the different regions is shown in Plate 8. The fractional contribution is calculated by weighting the average O_3 for each air mass type by its percentage of occurrence as observed during PEM-West A. At high latitudes the elevated O_3 in SINF dominated the O_3 budget (>80%) above 8 km, and continental

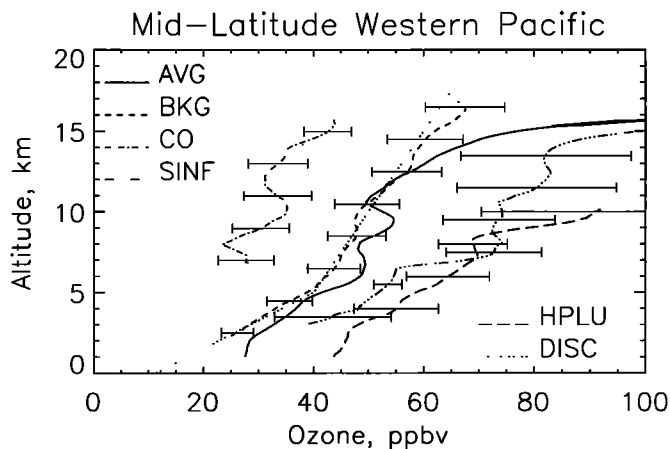


Figure 10. Average O_3 profile for western Pacific mid-latitude (20° - 40° N/ 110° - 150° E) region (solid line), and average O_3 profiles for background (medium-dashed line), convective outflow (long-short-dashed line), stratospherically influenced (long-short-short-dashed line), and high-ozone plume (long-dashed line) air masses shown relative to the reference O_3 profile, or discriminator (short-dashed line).

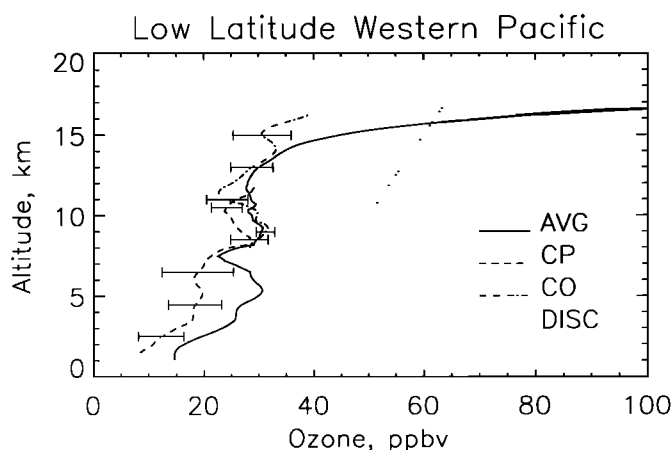


Figure 11. Average O_3 profile for western Pacific low latitude (0° - 20° N/ 110° - 150° E) region (solid line), and average O_3 profiles for clean Pacific (long-dashed line) and convective outflow (long-short-dashed line) air masses shown relative to the reference O_3 profile, or discriminator (short-dashed line).

plumes (BPLU and HPLU) dominated the O_3 budget over the rest of the troposphere. At midlatitudes, SINP contributed over 30% of the O_3 above 6 km, while continental plumes contributed over 40% below that altitude. The background air contributed about 35% of the O_3 over the entire free troposphere with minor contributions (less than ~20%) from the other air mass types. At low latitudes in the western Pacific the average O_3 is less than 30 ppbv up to 13 km (Figure 11), and the O_3 budget is dominated above 7 km (>85%) by the clean Pacific and convective outflow (marine) air mass types. Below 7 km, the clean Pacific air provided about 40% of the average O_3 , and CO-C and high- O_3 plumes contributed over 30% of the O_3 . In the central Pacific the background air accounted for more than 50% of the O_3 above 7 km, while below 6 km, SINP and high- O_3 plumes were a significant source of the O_3 (40-60%).

Chemical Characteristics of Different Air Masses

A detailed chemical characterization of the various air mass types encountered during PEM-West A was made using the comprehensive in situ measurement capabilities on the DC-8 [Hoell *et al.*, this issue]. Missions and time periods were identified that corresponded to cases where in situ sampling occurred within each air mass type characterized by the DIAL system (Table 6). These measurement periods primarily corresponded to level flight legs that had either been overflowed or underflowed in the same geographic region during wall-type missions. Table 6 also shows the altitudes and geographic locations of the measurements. Only one case of low- O_3 plumes (LPLU) and two cases of background- O_3 plumes (BPLU) and near surface air (NS) could be clearly identified as having been in situ sampled. While the DIAL classification scheme could readily identify these air mass types, the limited in situ sampling of these air masses must be recognized in the interpretation of their chemical characteristics. Table 7 gives a summary of the combined chemical signatures of each of the air mass types based on the in situ sampled cases. The average chemical composition derived for each air mass type represents the first attempt to relate the large-scale classification capabilities of the airborne DIAL system with the chemical signatures of these air masses.

The in situ measurements of background air (BKG) measurements were grouped primarily in the midtroposphere (5.2-8.6 km), while the plumes (BPLU, LPLU, and HPLU) were sampled over most of the lower troposphere (1.4-8.6 km). The clear cases of in situ measurements of stratospherically influenced air (SINF) were found in the mid to upper troposphere (8.6-11.0 km) at middle to high latitudes over the western Pacific and in the low to middle troposphere (3.4-4.6 km) at low latitudes over the central Pacific. The convective outflow-continental (CO-C) air was measured in the midtroposphere (7-8.6 km), and the clean Pacific (CP) air was measured in the low to midtroposphere (3.7-8.6 km). The convective outflow (CO) marine air was sampled in the upper troposphere (8.3-11.3 km). While the altitudes of these in situ measurements were generally consistent with the regions where the air masses were most often observed in the low to mid troposphere (<10 km), they cannot necessarily be considered to be representative of the same air mass type observed remotely by the DIAL system in the upper troposphere (~10-16 km). This is particularly true for SINP which has a chemical composition that is determined by significantly diluting air from the lower stratosphere with highly variable tropospheric air.

In general, many compounds follow the trends that might be expected for the different air masses. The chemical composition was similar for continental plumes with high O_3 levels (HPLU) and for continent convective outflow air (CO-C). Both had elevated average levels of O_3 (57-64 ppbv), CO (105-108 ppbv), CH_4 (1764-1777 ppbv), NO_y (645-679 pptv), SO_2 (124-127 pptv), PAN (99-161 pptv), NO_x (96-119 pptv), C_2H_6 (775-1122 pptv), C_2H_2 (189-230 pptv), ^{210}Pb (~11 fCi/m³ STP). These compounds are generally elevated in air from continental surface sources that have some pollution, and the backtrajectories also indicate that the observed air was from a continental source. The C_2H_2/CO and C_3H_8/C_2H_6 ratios in these air masses were also elevated (1.72-2.10 and 0.097-0.167, respectively) indicating that these air mass types have had a short processing time from their source over the continent. While the insoluble gas composition was similar in these air mass types, the levels of H_2O_2 (348 pptv) and CH_3OOH (146 pptv) were greatly reduced in the continental convective outflow (CO-C) air (444 and 141 pptv, respectively).

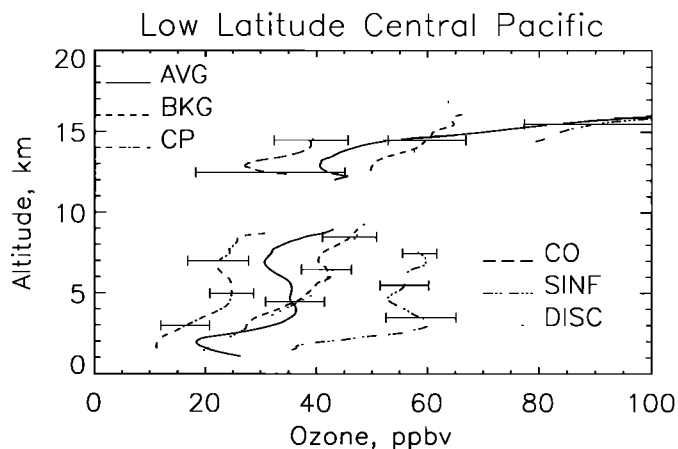


Figure 12. Average O_3 profile for low-latitude central Pacific (0° - 20° N/ 150° E- 160° W) region (solid line), and average O_3 profiles for background (medium-dashed line), clean Pacific (long-dashed line), and stratospherically influenced (long-short-short-short-dashed line) air masses relative to the reference O_3 profile, or discriminator (short-dashed line).

Table 2. Percentage of Troposphere With Stratospherically Influenced Air

Altitude, km	<i>Western Pacific*</i>			<i>Central Pacific†</i>
	0°-20°N Latitude	20°-40°N Latitude	40°-60°N Latitude	0°-20°N Latitude
17-18	99 (stratosphere)	100 (stratosphere)	---	100
16-17	76	90	---	97 (stratosphere)
15-16	22	51	100	74
14-15	0	44	100	13
13-14	0	38	100	1
12-13	0	35	100	1
11-12	1	27	100	0
10-11	1	22	100 (stratosphere)	0
9-10	1	27	87	0
8-9	0	15	71	0
7-8	0	6	36	4
6-7	0	5	20	10
5-6	0	7	5	26
4-5	0	1	0	23
3-4	0	2	0	16
2-3	0	0	0	14
1-2	0	0	0	23

*110°-150°E region except for high-latitude case, which is 150°E-160°W.

†150°E-160°W region.

Table 3. Percentage of Troposphere with Plumes

Altitude, km	<i>Western Pacific*</i>			<i>Central Pacific†</i>
	0°-20°N Latitude	20°-40°N Latitude	40°-60°N Latitude	0°-30°N Latitude
17-18	(stratosphere)	(stratosphere)	---	---
16-17	0	0	---	(stratosphere)
15-16	0	0	---	0
14-15	0	0	---	0
13-14	0	0	---	0
12-13	0	0	---	0
11-12	0	1	---	0
10-11	0	2	(stratosphere)	0
9-10	0	3	13	0
8-9	0	10	27	0
7-8	1	11	63	0
6-7	2	20	76	0
5-6	3	37	95	0
4-5	21	45	100	0
3-4	35	52	100	14
2-3	27	71	100	8
1-2	47	48	100	12

*110°-150°E region except for high-latitude case, which is 150°E-160°W.

†150°E-160°W region.

Ozone Trough

PEM West-A Flight 15 10 Oct 91

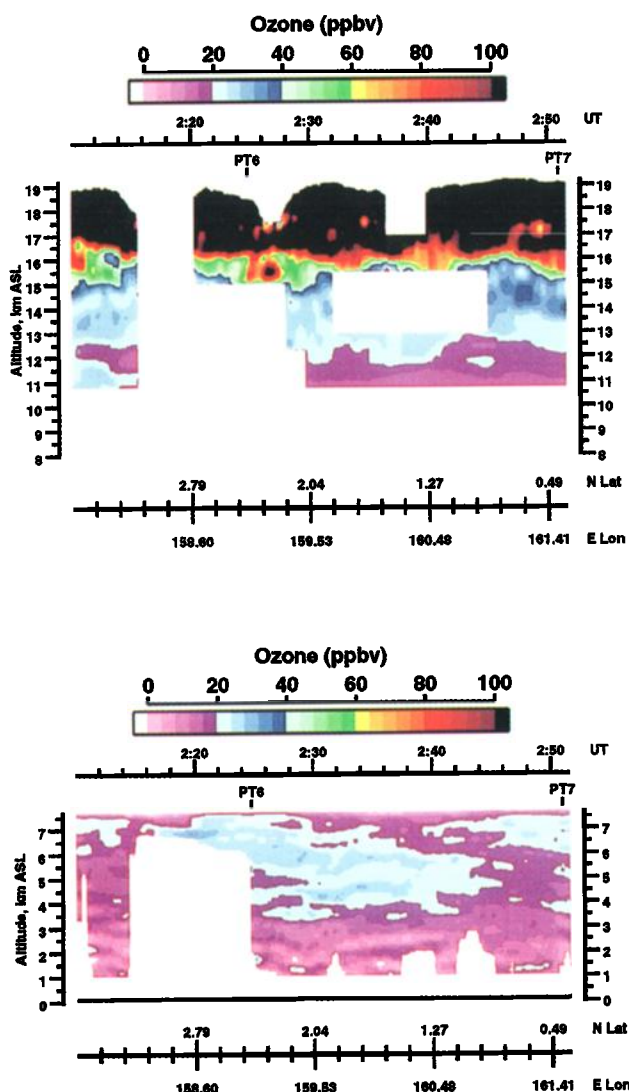


Plate 6. Nadir (bottom) and zenith (top) O_3 distributions associated with clean Pacific air observed near equator southeast of Guam on October 10, 1991 (PWA flight 15).

compared to the high- O_3 plumes (1030 and 435 pptv, respectively) due to the wet processing of the CO-C air during vertical convective transport over the land. The aerosols were also washed out of the CO-C air, as was evident in the low aerosol backscattering in the lidar returns, and this was also reflected in the low sulfate levels (13 pptv) in these air masses.

The chemical composition of the background O_3 plumes (BPLU) reflects the continental pollution source of the air with elevated CO (126 ppbv), SO_2 (163 pptv), NO_y (510 pptv), C_2H_6 (874 pptv), and H_2O_2 (4453 pptv). Due to the longer processing time, as indicated by a C_2H_2/CO ratio of ~ 1 , and the lower average altitude of the plumes, the O_3 in these plumes was within the range of our background O_3 criterion. The low O_3 observed in

some of the plumes (LPLU) was also associated with even longer processing times ($C_2H_2/CO \sim 0.84$; $C_3H_8/C_2H_6 \sim 0.076$) and possible photochemical loss of O_3 ; although there is some indication from the lower CO, SO_2 , NO_y , and hydrocarbon levels that there was less pollution in these plumes.

The stratospherically influenced air (SINF) had the lowest average levels of CO (71 ppbv), N_2O (305.9 ppbv), C_2H_6 (481 pptv), C_2H_2 (51.0 pptv), H_2O_2 (313 pptv), and nitrate (6.8 pptv) and the longest processing times as indicated by the low ratios of C_2H_2/CO (0.64) and C_3H_8/C_2H_6 (0.052). All of these factors reflect the influence of the stratospheric air on the composition of SINF. The average SINF composition includes three cases of directly sampled stratospheric air (Flights 4 and 5) and four cases where the stratospheric air that had been highly diluted with background tropospheric air (Flights 6, 19, and 20). Thus the variability of many species in the average SINF composition is not unique with respect to the other air mass types; however, gases that are low in the stratosphere were generally lower in SINF than in all but the clean Pacific (CP) and near-surface (NS) air. The unexpectedly high levels of SO_2 (214 pptv) and sulfate (390 pptv) in the average SINF composition is attributed to the presence of gas and aerosols in the stratospheric air from the Mount Pinatubo eruption in June 1991.

The clean Pacific and marine convective outflow (CO) air have similar chemical compositions for the insoluble species. In the case of marine convective outflow the levels of H_2O_2 and CH_3OOH are less than half that for CP. This results from the same wet scavenging process that reduces the soluble gases associated with the convective outflow of continental air (CO-C). In addition, sulfate is lower in the marine convective outflow from the washout of aerosols. Long processing times for the clean Pacific air is indicated by the low values of C_2H_2/CO (0.85) and C_3H_8/C_2H_6 (0.058) and the low levels of Q (27 ppbv), PAN (16.4 pptv), NO_y (140 pptv), NO_x (27.4 pptv), and hydrocarbons. Additional discussion of the chemical characteristics of these air mass types is given by Liu *et al.* [this issue] and Smyth *et al.* [this issue].

Conclusions

The troposphere over the Pacific during the late summer/early fall was found to be composed of a complex combination of different air masses. The distribution of O_3 and aerosols in these air masses has been used to differentiate between different air mass types. Backtrajectory analyses were used to identify the probable source (continental or marine) of the tropospheric air, and inference of stratosphere-troposphere exchange was made through PV analyses. The tropospheric composition was found to be greatly dependent on the region of the Pacific and the altitude range of the air masses. Nine types of large-scale air masses were characterized during PEM-West A. The spatial distribution, frequency of observation, and composition of these air masses were discussed above.

Significant enhancements in O_3 levels (typically $\geq 40\%$ greater than reference O_3 profile) were found at high latitudes (40° – 60° N) over the Pacific during the summer/fall due to photochemical O_3 production in continental plumes in the low to midtroposphere and to air that has been previously involved in stratospheric intrusions (SINF). Enhanced PV levels were associated with the SINF, and backtrajectory analysis confirmed the origin of the plumes over the Asian continent. The high- O_3 continental plumes and SINF represented 64% and 27%, respectively, of the troposphere in this high-latitude region.

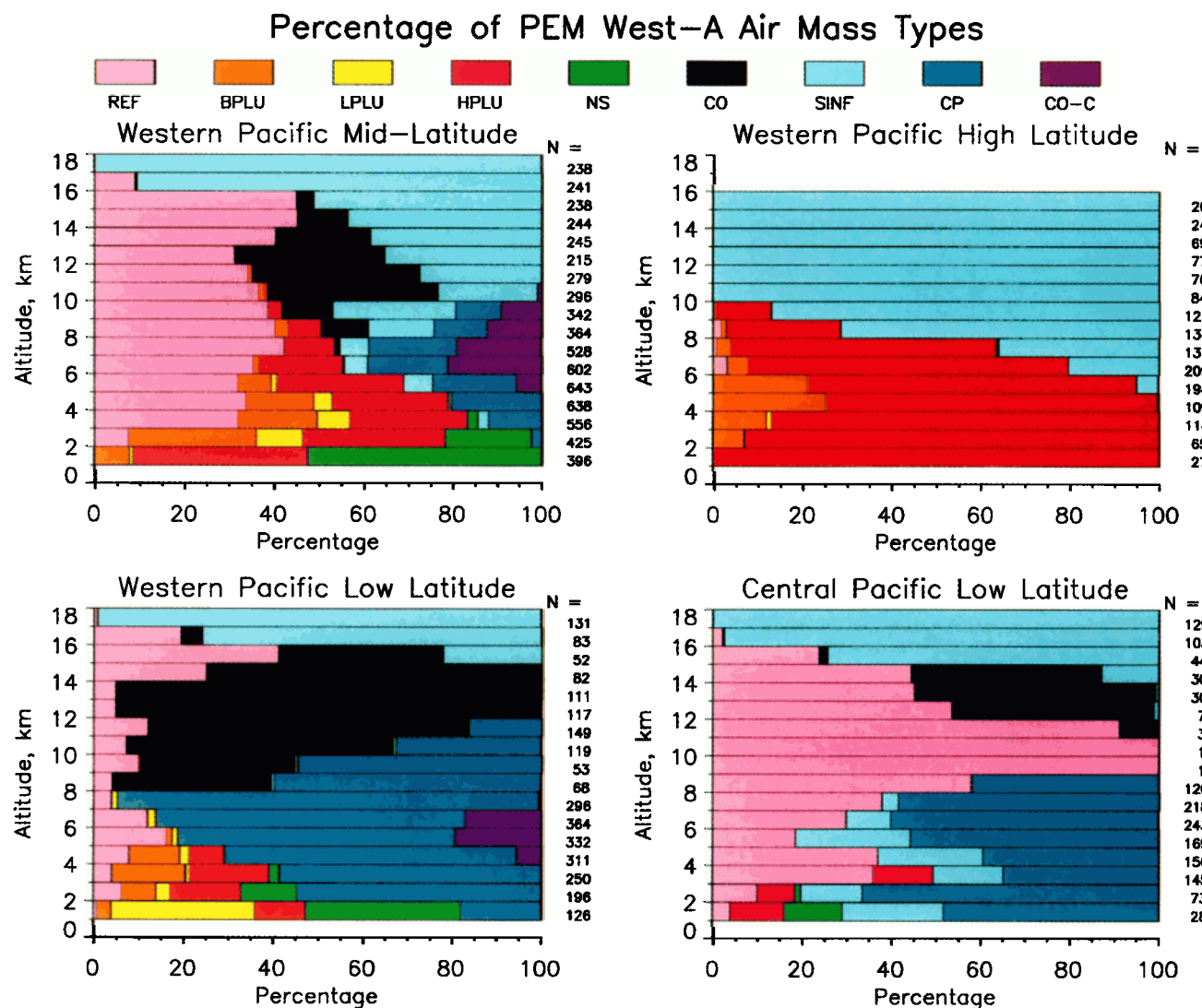


Plate 7. Percentage of time different air masses were observed over the Pacific in the indicated geographic and altitude regions. The air masses were categorized as either background air (REF/BKG), plumes with background O_3 (BPLU), plumes with low O_3 (LPLU), plumes with high O_3 (HPLU), near-surface (NS) air, convective outflows (CO) marine air, stratospherically influenced (SINF) air, clean Pacific (CP) air, or convective outflows continental (CO-C). The number of independent air mass classifications (N) that went into the analysis at each altitude is also given.

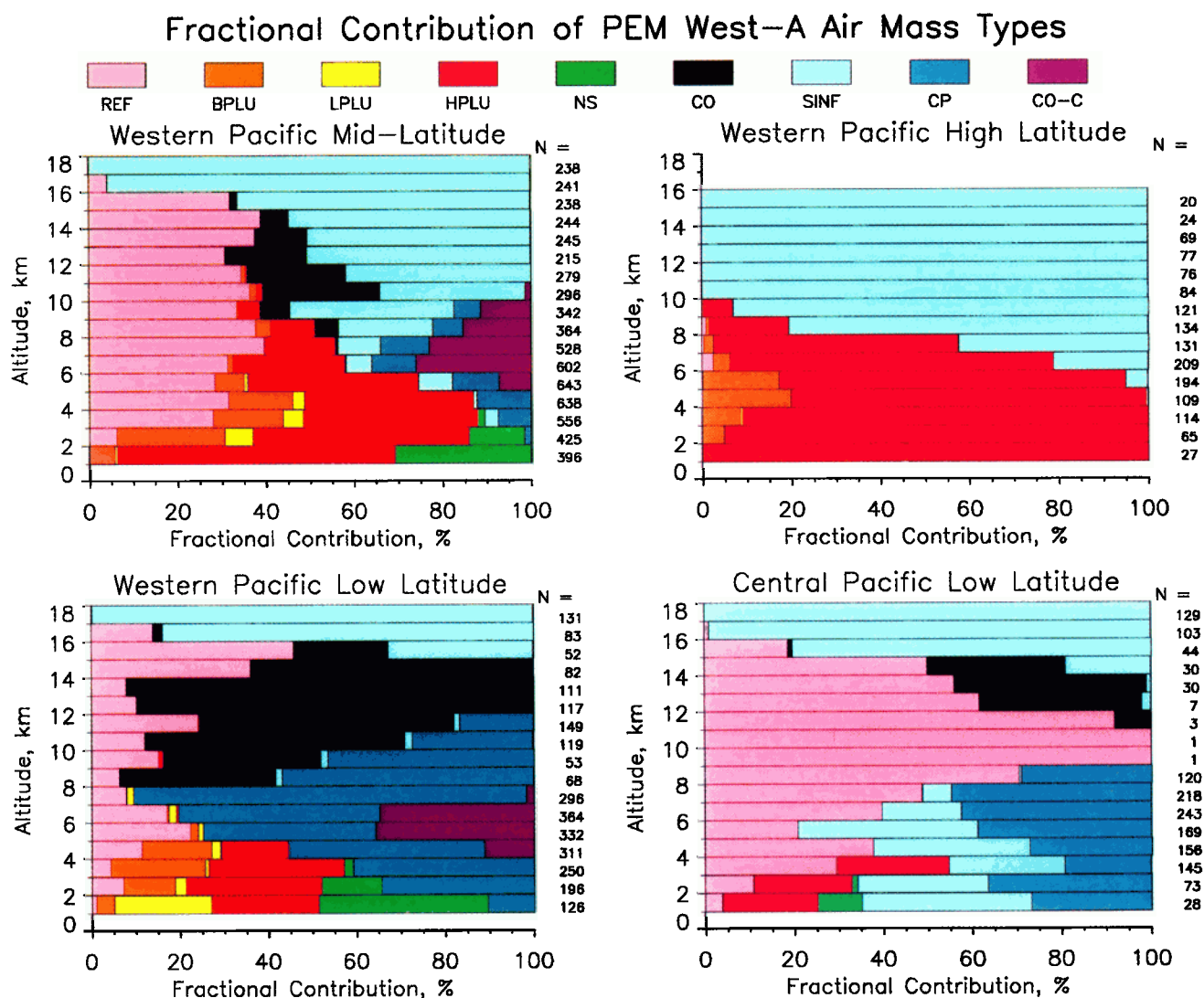


Plate 8. Fractional contribution (percentage) of different air mass types to the O_3 budget over the Pacific in the indicated geographic and altitude regions. The air mass types are the same as in Plate 7.

Table 4. Percentage of Troposphere With Clean Pacific or Convective Outflow (Marine) Air

Altitude, km	Western Pacific*			Central Pacific†
	0°-20°N Latitude	20°-40°N Latitude	40°-60°N Latitude	0°-30°N Latitude
17-18	(stratosphere)	(stratosphere)	---	---
16-17	5	0	---	(stratosphere)
15-16	37	4	---	2
14-15	75	11	---	43
13-14	95	21	---	54
12-13	95	34	---	45
11-12	87	37	---	---
10-11	92	38	(stratosphere)	---
9-10	89	21	0	---
8-9	95	22	0	42
7-8	94	21	0	58
6-7	69	18	0	60
5-6	62	19	0	56
4-5	65	20	0	39
3-4	58	12	0	35
2-3	55	2	0	66
1-2	18	0	0	48

*110°-150°E region except for high-latitude case, which is 150°E-160°W.

†150°E-160°W region.

Table 5. Average Percentage of Troposphere for Different Air Masses

Air Mass Type	Western Pacific*			Central Pacific†
	0°-20°N Latitude (0-17 km)	20°-40°N Latitude (0-17 km)	40°-60°N Latitude (0-10 km)	0°-30°N Latitude (0-16 km)
Background-free troposphere	11.3	31.4	0.8	45.9
Near surface	3.1	4.6	0.0	0.9
Plumes-background O ₃	2.5	5.3	8.0	0.0
Plumes-low O ₃	2.6	1.5	0.2	0.0
Plumes-high O ₃	3.4	12.1	63.7	2.3
Stratosphere influenced	6.5	23.6	27.4	13.9
Convective outflow-continental	2.6	4.0	0.0	0.0
Clean Pacific	36.3	7.0	0.0	26.8
Convective outflow-marine	31.6	10.5	0.0	10.1

*110°-150°E region except for high-latitude case, which is 150°E-160°W.

†150°E-160°W region.

Table 6. Air Mass In Situ Measurements

Air Mass Type*	Flight Number	1991	Times, UT	Altitude*, km	N. Latitude*, deg	E. Longitude*, deg
BKG	6	September 22	0505-0515	8.59	26.9	144.8
			0655-0707	6.13	27.6	146.1
	8	September 26	2143-2158	5.16	28.6	146.9
NS	6	September 22	0737-0811	0.29	28.1	146.8
	17	October 15	2127-2211	0.40	15.0	140.1
BPLU	16	October 13	0503-0515	1.38	5.5	128.7
			0520-0531	1.69	5.9	130.0
LPLU	12	October 4	0530-0540	3.66	25.1	122.4
HPLU	7	September 24	0420-0435	8.61	40.3	147.8
			0526-0602	3.39	37.3	146.8
			0620-0702	1.53	37.2	146.8
	13	October 6	0315-0323	4.57	27.1	127.4
SINF	4	September 16	2104-2124	10.54	55.8	-152.2
	5	September 17-18	2348-0047	10.99	48.3	159.3
		September 18	0053-0110	11.02	45.2	153.6
	6	September 22	0442-0445	8.59	28.7	147.9
			0448-0453	8.59	28.2	147.1
	19	October 19	0000-0008	4.57	17.7	-179.1
	20	October 20	1604-1615	3.38	19.7	-156.4
CO-C	8	September 26	1944-1954	8.59	29.4	146.9
	12	October 4	0400-0417	8.54	24.6	122.2
			0420-0434	8.54	22.5	121.4
	13	October 6	0310-0315	7.01	27.0	127.3
	14	October 8	0215-0315	8.30	18.4	120.1
CP	12	October 4	0456-0520	3.66	22.8	121.5
	15	October 11	0524-0555	6.14	6.1	154.4
	16	October 13	0551-0626	4.92	7.2	134.1
	17	October 15	2026-2042	8.59	15.0	141.1
			2227-2245	6.14	15.0	140.5
		October 15-16	2345-0021	6.14	14.9	139.9
	18	October 18	0101-0120	5.93	12.9	155.4
	20	October 20	1705-1720	4.91	19.4	-154.6
CO	12	October 4	0623-0630	10.12	24.6	122.2
	14	October 8	0325-0415	8.30	18.6	128.9
	15	October 13	0616-0701	11.04	10.2	148.5
	16	October 13	0727-0749	11.33	12.7	143.4

BKG—background or reference air; NS—near surface air; BPLU—plumes with background O₃ in the free troposphere; LPLU—plumes with low O₃ in the free troposphere; HPLU—plumes with high O₃ in the free troposphere; SINF—stratospherically influenced air; CO-C—convective outflow from convection over the continent; CP—clean Pacific air; CO—convective outflow from convection over the ocean.

*Average values.

At midlatitudes (20°–40°N) over the western Pacific the troposphere was dominated by background O₃ and aerosol conditions (31%); however, O₃ was enhanced due to stratospheric influences in 15–51% of the troposphere between 8 and 16 km. Plumes were frequently observed (over 37% of the time) in the lower troposphere below 5 km, and as in the high-latitude results, the majority of plumes had enhanced levels of photochemically produced O₃. These were due to advection of air from urban sources or biomass-burning regions. Low O₃ was found in association with cirrus clouds in up to 30% of the cases in 8- to 15-km region. This air was transported from near the surface into the upper troposphere as a result of convective storm activity over the Pacific.

At low latitudes (0°–20°N) in the western Pacific, low-O₃ air (up to 50% lower than reference O₃ profile) was found in 68% of the troposphere. The extensive vertical distribution of the low-O₃ air was attributed to convective storm activity associated with the many typhoons in this region of the Pacific during the late summer. Photochemical destruction of O₃ in the moist tropical marine atmosphere was responsible for the low O₃ ≤ 30 ppbv throughout most of the troposphere and the very low O₃ levels

(≤ 10 ppbv) below 2 km. In the central Pacific (150°E–160°W) at low latitudes the average O₃ levels were not so low as in the western Pacific. Background O₃ was observed over 46% of the troposphere, and clean Pacific air and convective outflows were found 37% of the time. Observations of enhanced O₃ in the lower troposphere (below 6 km) were unexpected. The low aerosol loading and enhanced PV values associated with this air confirmed that the enhanced O₃ was due to previous stratospheric intrusions. The SINF had probably resulted from stratospheric intrusions that occurred at midlatitudes over eastern Asia, and this air subsequently descended into the lower troposphere of the central Pacific around the anticyclonic circulation in the western South Pacific. Plumes with enhanced aerosols and enhanced O₃ (40–60 ppbv) were also observed in the lower troposphere over the central Pacific. These plumes were just above the marine boundary layer, and they were determined to have originated from distant fires in Borneo based on backtrajectory analyses and reports of extensive burning on the island.

The fractional contribution of the various air masses to the average O₃ profiles observed in the different regions was generally similar to the fractional occurrence of the air mass types

Table 7. Air Mass Composition (Average Value (s. d.)/ Median Value (Number of Cases) / Range of Values)

Air Mass Type (Number of Cases) ^a	BKG (3)	NS (2)	BPLU (2)	LPLU (1)	HPLU (4)	SINF (7)	CO-C (5)	CP (8)	CO (4)
Altitude, km	7.0/6.5	0.35	1.6	3.8	4.8/5.2	8.4/9.1	8.7/9.0	6.1/6.4	10.8/11.7
Dew Pt., °C	-24.6/-29.3	21.6	7.4	-0.4	-21.3/-17.2	-48.5/-44.2	-35.8/-37.4	-17.5/-14.3	-42.2/-43.8
O ₃ , ppbv	42.9/42.0	12.8	15.9	23.1	64.4/57.0	124.0/60.2	57.4/58.7	27.0/26.6	33.5/27.9
CO, ppbv	76.3/74.4	92.5	126.3	88.6	105.5/117.8	71.2/76.9	108.3/106.8	89.3/90.0	104.5/109.7
CH ₄ , ppbv	1723.9/1724.8	1718.0	1688.6	1713.8	1764.0/1777.2	1709.8/1726.0	1777.5/1769.8	1709.9/1712.3	1729.6/1723.0
N ₂ O, ppbv	308.99 (1)	309.34 (1)	308.77 (1)	309.25	309.20/309.47	305.93/309.13 (4)	309.53/309.54	309.05/309.04	309.08/309.17
SO ₂ , pptv	61.9/66.0 (2)	55.4	163	42.0	124/139 (3)	214/226 (6)	127.2/128.3	59.0/51.4	98.3/98.6
CS ₂ , pptv	6.87/8.14 (2)	3.55	0.90	2.80	4.17/3.14 (3)	2.98/2.58 (5)	3.07/1.64	0.68/0.75	1.49/1.17
PAN, pptv	45.5 (2)	2.0	2.0	34.2	161/177	71.5/58.7	99.1/103.8	16.4/17.2	34.4/19.0
C ₂ Cl ₄ , pptv	3.92 (2)	3.58	1.35	2.80	6.77/6.80	4.12/4.13	3.34/3.02	2.96/2.53	3.02/2.92
NO _y , pptv ^b	334/341	178	510	319	679/711	439/555 (4)	645/603	233/259 (6)	488 (2)
NO ₃ , pptv ^c	273/263	—	116	—	464/488	368/307	402/375	140/143	234/288
NO _x , pptv	78.9 (2)	26.4	19.8	35.4	95.7/123.1	65.2/91.5 (4)	118.8/118.2	27.4/28.8	86.3/73.0 (3)
CH ₃ CCl ₃ , pptv	119.5/121.5	124.7	113.3	135.0	132.8/139.3	124.7/132.4 (5)	121.8/124.1	124.6/126.2	127.0/129.6
C ₂ H ₆ , pptv	492/488	507	874	539	1122/1122	481/542 (6)	775/775	573/623	661/682
C ₂ H ₄ , pptv	13.6/13.5	19.9	29.8	14.3	53.4/43.7	20.7/21.2 (6)	15.9/14.4	14.6/12.0	16.3/14.8
C ₂ H ₂ , pptv	56.5/59.0	73.7	131.9	73.0	230/301	51.0/53.0 (6)	189/194	76.8/93.9	122.3/101.6
C ₃ H ₈ , pptv	21.2/16.5	23.6	82.0	42.0	199/265	26.3/24.5 (6)	75.9/69.7	34.1/36.3	50.0/40.4
C ₄ H ₆ , pptv	14.0/10.0	27.0	43.1	24.0	58.8/76.7	13.0/19.5 (4)	37.1/34.2	19.0/18.2	17.9/21.0
H ₂ O ₂ , pptv	566/393	1562	4453	1839	1030/1414	313/152 (6)	444/415	1185/871 (7)	559 (2)
CH ₃ OOH, pptv	272/214	1419	2171	823	435/586	219/149 (6)	141/145	774/636 (7)	258 (2)
Aerosols, cm ⁻³	65.7 (1)	176.7	94.7	—	31.3 (1)	—	—	25.8 (2)	—
Sulfate, pptv	—	222	382 (1)	—	126 (2)	390 (2)	13 (1)	34 (2)	14 (1)
Nitrate, pptv	—	17.5	95.9 (1)	—	45.6 (2)	6.8 (2)	37.0 (1)	18.0 (2)	63.0 (1)
⁷ Be, fCi/scm	—	144	81 (1)	—	201 (2)	4444 (2)	104 (1)	99 (2)	187 (1)
²¹⁰ Pb, fCi/scm	—	5.5	5.8 (1)	—	11.5 (2)	—	11.0 (1)	1.3 (2)	0.98 (1)
C ₂ H ₂ /CO ^d	0.73/0.79	0.75	1.03	0.84	2.10/2.36	0.64/0.69 (6)	1.72/1.80	0.85/0.92	1.23/1.03 (4)
C ₃ H ₈ /C ₂ H ₆ ^e	0.042/0.034	0.042	0.091	0.076	0.167/0.177	0.052/0.045 (6)	0.097/0.090	0.058/0.060	0.072/0.074

^aNumber of cases averaged together and used for median (three or more cases only), and if fewer cases are used, the number is indicated in the parenthesis; ^bGeorgia Institute of Technology; ^cNagoya University; ^dppbv/ppbv; ^e pptv/pptv.

in that region; however, the higher O₃ levels in the SINP and high-O₃ plume air masses resulted in these air mass types having an enhanced contribution to the average O₃ profile at the expense of air mass types that have low O₃ levels, such as the clean Pacific and marine convective outflow air. At high latitudes, air from the lower stratosphere dominated the O₃ profile above 8 km, and high O₃ associated with high aerosols in continental outflow plumes dominated the O₃ profile in the low to midtroposphere. At midlatitudes in the western Pacific, SINP contributed over 35% of the O₃ above 6 km, and this is significant since the tropopause is above 16 km in this region. Many different types of air masses contributed to the average O₃ profile below 6 km; however, the high-O₃ plume air made the most significant (40-65%) influence on the O₃ level. With the predominant easterly flow at the low latitudes the average O₃ profile was low (typically <30 ppbv), and the clean Pacific and convective outflow air mass types determined the O₃ profile above 7 km, and in the lower troposphere the contribution of the clean Pacific air decreased with altitude to less than 35% at 2 km. Below 5 km, plumes from various continental sources (enhanced aerosols and O₃) combine to influence the average O₃ profile. A very surprising result was found in the central Pacific at low latitudes. While the background and clean Pacific air mass types dominated the average O₃ profile above 6 km, the air associated with SINP was found to have contributed 27 to 40% of the average O₃ below 6 km. This shows the unexpected importance of this enhanced O₃ source to the O₃ budget in this remote region of the Pacific.

In general, the average chemical composition of all the air mass types followed trends that either reflected anthropogenic influences from continental sources, stratospheric influences or long processing times over the tropical marine environment. Convective transport processes over the land and the ocean tended to decrease soluble gases and washout aerosols; however, the insoluble species remained to reflect the near-surface source of the air. Thus the continental convective outflow air resembled the insoluble composition of the continental plume air, and the marine convective outflow air resembled the insoluble composition of the clean Pacific air. With the exception of the stratospherically influenced air the average O₃ levels in the different air mass types were generally inversely related to the amount of processing of the air as defined by the C₂H₂/CO ratio. The amount of air mass processing (i.e., photochemistry plus mixing) significantly influenced the composition of the observed air masses [Liu *et al.*, this issue; Smyth *et al.*, this issue]. As was done for O₃, the contribution of various air mass types to the tropospheric budget of other compounds can be determined from the chemical composition and fractional occurrence information presented in this paper for each air mass type.

Acknowledgments. The authors express their appreciation to Bill McCabe, Jerry Williams, Neale Mayo, and Byron Meadows for their support in operating the airborne DIAL system in the field for the measurement of O₃ and aerosol distributions. We also thank Syed Ismail, Greg Nowicki, Shane Mayor, and Susan Kooi for their assistance in the reduction of the DIAL data and Yong Zhu (MIT) for the PV figure preparation. We appreciate the cooperation of the NASA Ames Research Center's DC-8 flight crew in conducting this mission and the assistance of the European Center for Medium-Range Weather Forecasting for providing the potential vorticity analysis. This research was supported by the NASA Global Tropospheric Chemistry Program.

References

- Anderson, B. E., G. L. Gregory, J. E. Collins, G. W. Sachse, and T. J. Conway, Airborne observations of the spatial and temporal variability of tropospheric carbon dioxide, *J. Geophys. Res.*, this issue.
- Bachmeier, A. S., R. E. Newell, M. C. Shipman, Y. Zhu, D. R. Blake, and E. V. Browell, PEM-West A: Meteorological overview, *J. Geophys. Res.*, this issue.
- Blake, D. R., T.-Y. Chen, T. W. Smith Jr., C. J.-L. Wang, D. W. Wingenter, N. J. Blake, F. S. Rowland, and E. W. Mayer, Three-dimensional distribution of NMHCs and halocarbons over the northwestern Pacific during the 1991 Pacific Exploratory Mission (PEM-West A), *J. Geophys. Res.*, this issue.
- Browell, E. V., Remote sensing of tropospheric gases and aerosols with an airborne DIAL system, in *Optical Laser Remote Sensing*, edited by D. K. Killinger and A. Mooradian, pp. 138-147, Springer-Verlag, New York, 1983.
- Browell, E. V., Differential absorption lidar sensing of ozone, *Proc. IEEE*, 77, 419-432, 1989.
- Browell, E. V., A. F. Carter, S. T. Shipley, R. J. Allen, C. F. Butler, M. N. Mayo, J. H. Siviter Jr., and W. M. Hall, NASA multipurpose airborne DIAL system and measurements of ozone and aerosol profiles, *Appl. Opt.*, 22, 522-534, 1983.
- Browell, E. V., S. Ismail, and S. T. Shipley, Ultraviolet DIAL measurements of O₃ profiles in regions of spatially inhomogeneous aerosols, *Appl. Opt.*, 24, 2827-2836, 1985a.
- Browell, E. V., S. T. Shipley, C. F. Butler, and S. Ismail, Airborne lidar measurements of aerosols, mixed layer heights, and ozone during the 1980 PEPE/NEROS summer field experiment, *NASA Ref. Publ.*, RP-1143, 1985b.
- Browell, E. V., E. F. Danielsen, S. Ismail, G. L. Gregory, and S. M. Beck, Tropopause fold structure determined from airborne lidar and in situ measurements, *J. Geophys. Res.*, 92, 2112-2120, 1987.
- Browell, E. V., C. F. Butler, S. A. Kooi, M. A. Fenn, R. C. Harriss, and G. L. Gregory, Large-scale variability of ozone and aerosols in the summertime Arctic and subarctic troposphere, *J. Geophys. Res.*, 97, 15, 16,433-16,450, 1992.
- Browell, E. V., M. A. Fenn, C. F. Butler, W. B. Grant, R. C. Harriss, and M. C. Shipman, Ozone and aerosol distributions in the summertime troposphere over Canada, *J. Geophys. Res.*, 99, 1739-1755, 1994.
- Collins, J. E., G. W. Sachse, B. E. Anderson, R. C. Harriss, S. Sandholm, L. O. Wade, L. G. Burney, and G. F. Hill, Airborne nitrous oxide observations over the western Pacific Ocean: September-October 1991, *J. Geophys. Res.*, this issue.
- Danielsen, E. F., Stratospheric source for unexpectedly large values of ozone measured over the Pacific Ocean during Gametag, August 1977, *J. Geophys. Res.*, 85, 401-412, 1980.
- Danielsen, E. F., and R. S. Hipskind, Stratospheric-tropospheric exchange at polar latitudes in summer, *J. Geophys. Res.*, 85, 393-400, 1980.
- Davis, D. D., Project Gametag: An overview, *J. Geophys. Res.*, 85, 7285-7292, 1980.
- Davis, D. D., et al., Assessment of ozone photochemistry in the western North Pacific as inferred from PEM-West A observations during fall 1991, *J. Geophys. Res.*, this issue (b).
- Gatz, D. F., A review of chemical tracer experiments on precipitation systems, *Atmos. Environ.*, 11, 945-953, 1977.
- Gregory, G. L., A. S. Bachmeier, D. R. Blake, B. G. Heikes, D. C. Thornton, J. D. Bradshaw, and Y. Kondo, Chemical signatures of aged Pacific marine air: Mixed layer and free troposphere as measured during PEM-West A, *J. Geophys. Res.*, this issue.
- Heikes, B. G., Hydrogen peroxide and methylhydroperoxide distributions related to ozone and odd hydrogen over the North Pacific in the fall of 1991, *J. Geophys. Res.*, this issue.
- Hoell, J. M., Jr., D. L. Albritton, G. L. Gregory, R. J. McNeal, S. M. Beck, R. J. Bendura, and J. W. Drewry, Operational overview of NASA GTE/CITE 2 airborne instrument intercomparisons: Nitrogen dioxide, nitric acid, and peroxyacetyl nitrate, *J. Geophys. Res.*, 95, 10,047-10,054, 1990.
- Hoell, J. M., et al., Pacific Exploratory Mission-West A (PEM-West A): September-October 1991, *J. Geophys. Res.*, this issue.
- Johnson, J. E., V. M. Koropalov, K. E. Pickering, A. M. Thompson, N. Bond, and J. W. Elkins, Third Soviet-American Gas and Aerosol (SAGA 3) experiment: Overview and meteorological and oceanographic conditions, *J. Geophys. Res.*, 98, 16,893-16,908, 1993.
- Liu, S. C., M. McFarland, D. Kley, O. Zafiriou, and B. Huebert, Tropospheric NO_x and O₃ budgets in the equatorial Pacific, *J. Geophys. Res.*, 88, 1360-1368, 1983.
- Liu, S. C., et al., Model study of tropospheric trace species distributions during PEM-West A, *J. Geophys. Res.*, this issue.
- Merrill, J. T., R. Bleck, and L. Avila, Modeling atmospheric transport to the Marshall Islands, *J. Geophys. Res.*, 90, 12,927-12,936, 1985.
- Merrill, J. T. et al., Trajectory results and interpretation for PEM-West A, *J. Geophys. Res.*, this issue.

- Newell, R. E., et al., Atmospheric sampling of supertyphoon Mireille with the NASA DC-8 aircraft on September 27, 1991, during PEM-West A, *J. Geophys. Res.*, this issue.
- Pickering, K. E., R. R. Dickerson, W. T. Luke, and L. J. Nunnermacher, Clear-sky vertical profiles of trace gases as influenced by upstream convective activity, *J. Geophys. Res.*, *94*, 14,879-14,892, 1989.
- Pickering, K. E., A. M. Thompson, J. R. Scala, W. K. Tao, J. Simpson, and M. Garstang, Photochemical ozone production in tropical squall line convection during NASA/GTE/ABLE 2A, *J. Geophys. Res.*, *96*, 3099-3114, 1991.
- Ridley, B. A., and F. Robinson, The Mauna Loa Observatory Photochemistry Experiment, *J. Geophys. Res.*, *97*, 10,285-10,290, 1992.
- Routhier F., and D. D. Davis, Free tropospheric/boundary-layer airborne measurements of H₂O over the latitude range of 58°S to 70°N: Comparison with simultaneous ozone and carbon monoxide measurements, *J. Geophys. Res.*, *85*, 7293-7306, 1980.
- Savoie, D. L., and J. M. Prospero, Comparison of oceanic and continental sources of non-sea-salt sulfate over the Pacific Ocean, *Nature*, *339*, 685-687, 1989.
- Singh, H. B., et al., Peroxyacetyl nitrate measurements during CITE 2: Atmospheric distribution and precursor relationships, *J. Geophys. Res.*, *95*, 10,163-10,178, 1990.
- Singh, H. B., et al., Reactive nitrogen and ozone over the western Pacific: Distribution, partitioning, and sources, *J. Geophys. Res.*, this issue.
- Smyth, S., et al., Comparison of free tropospheric Western Pacific air mass classification schemes for the PEM-West A experiment, *J. Geophys. Res.*, this issue.
- Thornton, D. C., et al., Sulfur dioxide as a source of condensation nuclei in the upper troposphere of the Pacific Ocean, *J. Geophys. Res.*, this issue.
- Zhou, M., N. Lu, J. Miller, F. P. Parungo, C. Nagamoto, and S.-J. Yang, Characterization of atmospheric aerosols and of suspended particles in seawater in the western Pacific Ocean, *J. Geophys. Res.*, *97*, 7553-7567, 1992.
- B. E. Anderson, E. V. Browell, W. B. Grant, G. L. Gregory, and G. W. Sachse, Atmospheric Sciences Division, NASA Langley Research Center, Mail Stop 401A, Hampton, VA 23681-0001.
- A. R. Bandy and D. C. Thornton, Drexel University, Philadelphia, PA 19104.
- D. R. Blake and F. S. Rowland, University of California, Irvine, CA 92717.
- J. D. Bradshaw, D. D. Davis, and S. T. Sandholm, Georgia Institute of Technology, Atlanta, GA 30332.
- A. S. Bachmeier, C. F. Butler, and M. A. Fenn, Science Applications International Corporation, Hampton, VA 23666.
- B. G. Heikes and J. T. Merrill, University of Rhode Island, Narragansett, RI 02882.
- Y. Kondo, Nagoya University, Toyokawa, Aichi, Japan.
- S. C. Liu, NOAA Aeronomy Laboratory, Boulder, CO 80303.
- R. E. Newell, Massachusetts Institute of Technology, Cambridge, MA 02139.
- H. B. Singh, NASA Ames Research Center, Moffett Field, CA 94035.
- R. W. Talbot, University of New Hampshire, Durham, NH 03824.

(Received August 5, 1994; revised July 8, 1995;
accepted July 14, 1995.)